Economic Geology, v. 117, no. 7, pp. 1481–1496

A Role for Crustal Assimilation in the Formation of Copper-Rich Reservoirs at the Base of Continental Arcs

Santiago Tassara† and Jay J. Ague

Department of Earth and Planetary Sciences, Yale University, New Haven, Connecticut 06520-8109, USA

Abstract

Understanding the behavior of chalcophile elements during the evolution of arc magmas is critical to refining models for the formation and distribution of porphyry copper deposits used in mineral exploration. Because magmas in continental arcs undergo copper depletion during their early differentiation, a widely held hypothesis posits that the removed copper is locked at the base of the crust in copper-rich cumulates that form due to early sulfide saturation. Testing this hypothesis requires direct evidence for such copper-rich reservoirs and a comprehensive understanding of the mechanisms driving sulfide saturation. Interaction between oxidized magmas and reducing crustal material in island arcs has been shown to be an efficient process causing sulfide saturation. However, the extent to which crustal assimilation impacts the flux of chalcophile elements during magmatism in thick continental arcs remains to be established. Here, we provide a deep perspective into these problems by studying a suite of subarc cumulate rocks from the Acadian orogen, New England (USA). These cumulates record the imprint of subduction zone magmatism and represent the residues left behind during the genesis of intermediate to evolved Acadian magmas (ca. 410 Ma). We find that the most primitive Acadian cumulates are enriched in copper (up to ~730 μg g^{-1}) hosted by sulfide phases, providing direct evidence for the formation of lower crustal copper-rich reservoirs. The Acadian cumulates reveal a wide range of $\delta^{34}S$ values, from –4.9‰ in the ultramafic rocks to 8‰ in the most evolved mafic rocks. The negative $\delta^{34}S$ values observed in the most primitive and copper-rich cumulates (avg –3‰) reflect the assimilation of isotopically light sulfur from surrounding sulfidic and graphite-bearing metasedimentary rocks ($\delta^{34}S$ of –19 to –12‰), whereas the more evolved cumulates with positive $\delta^{34}S$ signatures may have formed from different magma batches that experienced less sediment assimilation. The assimilation of these reducing metasedimentary rocks caused a critical drop in oxygen fugacity (~ΔFMQ –2.5 to –1.9; FMQ = fayalite-quartz-magnetite buffer) in the evolving magmas, ultimately leading to extensive sulfide saturation and the consequent formation of copper-rich subarc cumulates. Assimilation-driven sulfide saturation may be a common process at the root of thickened arc crusts that triggers the formation of lower crustal copper-rich reservoirs, which play a pivotal role in the fate of copper during arc magmatism. Thus, deeply buried reducing metasedimentary crustal material at the base of continental arcs can act as a barrier to the magmatic flux of chalcophile elements and may play a crucial role in the genesis and distribution of porphyry copper deposits.

Introduction

Thick continental arcs above subduction zones are key sites on Earth where the most massive anomalies of copper (Cu) and sulfur (S) occur (i.e., porphyry Cu deposits; Sillitoe, 1972, 2010; Richards, 2003). These deposits are intimately associated with oxidized and water-rich arc magmatism (Hedenquist and Lowernstern, 1994; Richards, 2015). Paradoxically, an increasing body of evidence indicates that continental arc magmas evolve toward low concentrations of Cu—and other chalcophile elements—during magmatic differentiation throughout the arc lithosphere (Jenner et al., 2010; Lee et al., 2012; Chiaradia, 2014; Richards, 2015; Jenner, 2017; Cox et al., 2019, 2020). The decreasing Cu in these magmas has been largely attributed to sulfide saturation during ascent and differentiation. Under such scenarios, owing to its chalcophile behavior, Cu is predicted to be sequestered by segregated magmatic sulfide phases (Jenner et al., 2010; Lee et al., 2012; Jenner, 2017; Wang et al., 2018; Chen et al., 2020; Li, Y., et al., 2021). However, the exact mechanisms driving sulfide saturation and the fate of the missing Cu in evolving arc magmas remain unclear.

A recent view holds that sulfides are lost as minor disseminations within the dominant proportion of plutonic rocks that crystallize at various depths as magmas ascend and evolve throughout the lithosphere (Richards, 2015). An alternative hypothesis suggests that segregated magmatic sulfides are efficiently collected in sulfide- and Cu-rich subarc cumulates (Lee et al., 2012; Chiaradia, 2014; Jenner, 2017; Chen et al., 2020). The formation of such Cu-rich reservoirs at the base of the arc crust may play an important role in the genesis of magmatic-hydrothermal ore deposits. For instance, although small amounts of magmatic sulfide saturation may not affect the porphyry Cu forming potential (Cocker et al., 2015; Hao et al., 2019; Du and Audétat, 2020; Park et al., 2021), significant sulfide saturation is considered detrimental to the genesis of synmagmatic porphyry Cu deposits because it clearly limits the flux of ore-forming elements to shallow crustal levels (Jenner et al., 2010; Park et al., 2015, 2019; Richards, 2015; Hao et al., 2017). However, Cu-rich cumulates that formed after significat sulfide saturation may also act as an important reservoir and source of ore-forming metals for subsequent tectonic and magmatic events to generate unusually metal-rich magmas parental to giant syn- and/or postsubduction porphyry-type deposits (e.g., Core et al., 2006; Chiaradia et al., 2009, 2014; Richards, 2009; Jenner et al., 2010; Sillitoe, 2012; Wilkinson, 2013; Holwell et al., 2022). Therefore, a more comprehensive understanding of the deep-seated petrogenetic processes that control sulfide saturation and the behavior of Cu and other

†Corresponding author: e-mail, santiago.tassara@yale.edu

 Submitted: October 27, 2021 / Accepted: February 24, 2022

chalcophile elements during continental arc magmatism is critical to advancing our knowledge of the genesis and distribution of ore deposits in arc-related settings.

Experimental studies in mafic silicate melts have shown that increasing pressure and decreasing temperature decrease S solubility (Mavrogenes and O'Neill, 1999; O'Neill and Mavrogenes, 2002). In addition, decreasing FeO content also decreases S solubility (Liu et al., 2007; Baker and Moretti, 2011). Furthermore, whereas sulfide (S^{2-}) is the dominant S species in silicate melts under relatively reduced conditions, the oxidized and more soluble sulfate (S^{6+} in SO_4^{2-}) dominates under oxidizing conditions (Li and Ripley, 2005; Jugo, 2009; Matjuschkin et al., 2016). Hence, elevated oxygen fugacities (f_{O_2}) in silicate melts result in increasing S^{6+}/S_{tot} ratios and high S solubility, hindering sulfide saturation. Recently proposed models for the genesis of Cu-rich cumulates after sulfide saturation in arc magmas that evolve in thick continental crusts build upon the above-mentioned experimental constraints and include (1) high pressures imprinted by the overriding plate in thick arcs (Matjuschkin et al., 2016; Jenner, 2017; Cox et al., 2019), (2) decreasing FeO of evolving calc-alkaline magmas during differentiation (Chen et al., 2020; Barber et al., 2021), and (3) relatively low f_{O_2} conditions that could either be a primary feature of subarc mantle melts (Lee et al., 2012) or be attained after the onset of early magnetite crystallization (Chiaradia, 2014). These models dominantly envisage a crystal fractionation-driven behavior of S and chalcophile elements during arc magmatism. However, it has been shown that open-system mixing and assimilation of lower crustal rocks is a nearly ubiquitous process that exerts an important control on the geochemistry of continental arc magmas (e.g., DePaolo, 1981; Ague and Brimhall, 1987, 1988; Hildreth and Moorbath, 1988; Annen et al., 2006; DeCelles et al., 2009; Walker et al., 2015). Importantly, Tomkins et al. (2012) demonstrated the potential of crustal assimilation processes to cause reduction-induced sulfide saturation and the genesis of Ni-Cu sulfide deposits in island-arc settings. The advantage posed by this hypothesis is that magmatic reduction provides a strong mechanism for extensive sulfide precipitation and thus an increased potential to form Cu-rich cumulates (Richards, 2015). Although this process has been shown to form Ni-Cu sulfide deposits in the relatively thin crust of island arcs (<25-km depth; Tomkins et al., 2012; Wei et al., 2019), the extent to which it operates and leads to the formation of Cu-rich cumulates at the base of thicker continental arcs (>30 km) remains to be established.

To address this prominent gap in knowledge, we explore the behavior of Cu during arc magmatism by focusing on a suite of hydrous ultramafic to mafic cumulates from the Acadian in southern New England (Connecticut, USA) (Fig. 1). These cumulates represent the subarc roots of the Acadian orogen (Devonian) and are genetically linked to most of the coeval intermediate to silicic magmatism in New England (Tassara et al., 2021). Thus, they provide an exceptional opportunity to directly explore the behavior of Cu in continental-arc magmas during their early differentiation in the deep crust. We integrate detailed sulfide petrography, bulk-rock lithophile trace elements, Cu and Ni concentrations, bulk-rock S isotope analyses, and mineral chemistry. The results suggest that crustal assimilation may trigger extensive sulfide saturation and, thus, exert a key control in the formation of Cu-rich cumulates during arc magmatism.

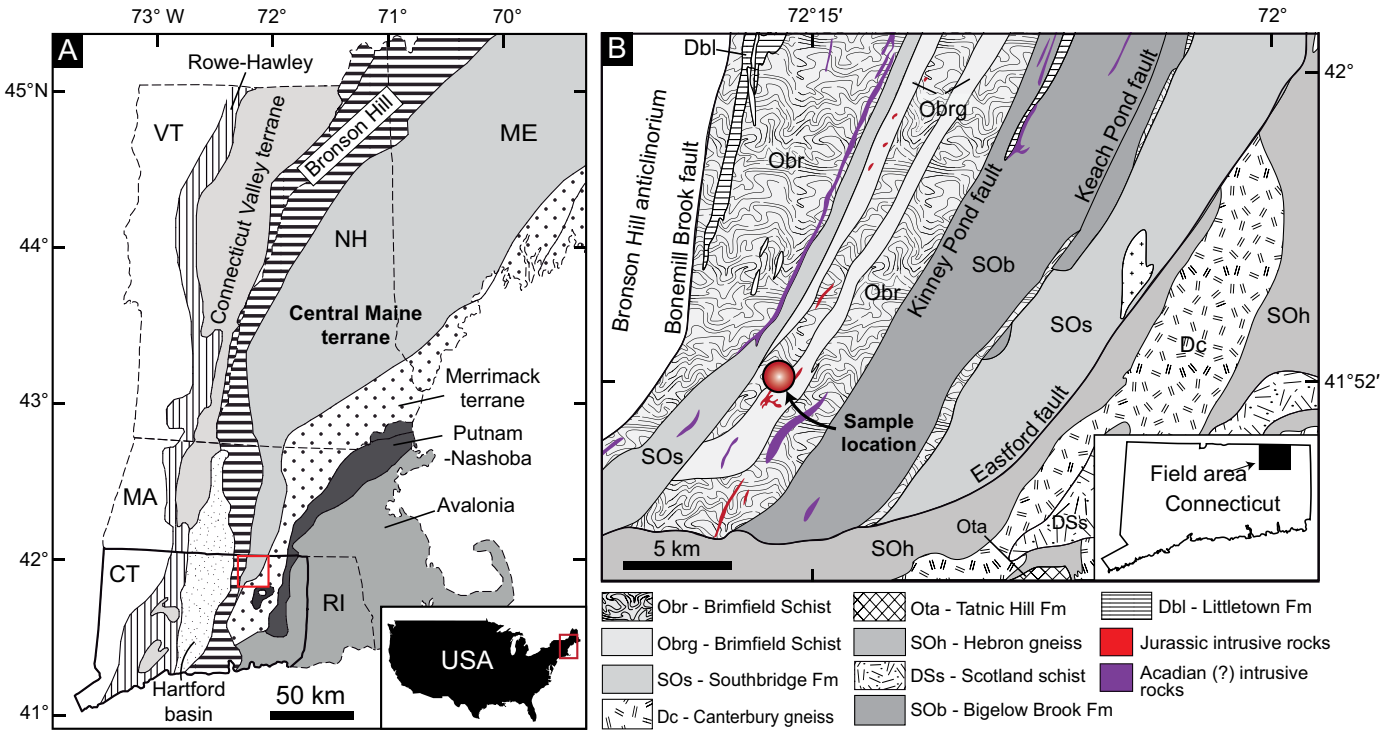

Fig. 1. (A) Geologic map of New England and its major lithotectonic units. CT = Connecticut, MA = Massachusetts, ME = Maine, NH = New Hampshire, RI = Rhode Island, VT = Vermont. (B) Detailed geologic map of the field area in northeastern Connecticut (after Rodgers, 1985). Major thrust faults are labeled. The red circle indicates the sample location.

Geologic Background and Samples

The Appalachians are an accretionary orogen that developed along the eastern margin of Laurentia during the Paleozoic era throughout a complete Wilson cycle that started with the breakup of the supercontinent Rodinia and culminated with the assembly of the supercontinent Pangea (Hatcher, 2010). In the northern Appalachians (Fig. 1), this orogenic history resulted from the collision and complex amalgamation of arcs and crustal blocks of peri-Laurentian and subsequent peri-Gondwanan microcontinents before the constitution of Pangea (van Staal et al., 2009). The Acadian orogeny (~423–385 Ma) is a crust-forming event characterized by intense deformation, metamorphism, and synchronous magmatism that resulted from the closure of the Iapetus Ocean and the impingement and collision of microcontinent Avalonia to the western margin of composite Laurentia (van Staal et al., 2009).

The studied rocks are olivine-pyroxene hornblendites, olivine-hornblende pyroxenites, norites and/or orthopyroxenites, hornblendites (hereafter ultramafics), and gabbros and anorthosite veins (hereafter mafics). They lie within a recently discovered mélange complex in northeastern Connecticut, southern New England (Tassara et al., 2021; Fig. 1). The mélange complex occurs along thrust faults that crosscut the Brimfield Schist in the Central Maine terrane, a lithotectonic unit of the Acadian orogen in New England (Fig. 1). Related rocks of the Brimfield Schist and its internal shear zones record episodes of metamorphism during the Acadian and Neoacadian (ca. 360 Ma) events. Metamorphic conditions recorded in silica-undersaturated and silica-saturated metapelitic rocks reached ultrahigh-temperature and high-pressure granulite conditions (>1,000°C, ~1.8 GPa), indicating that the thrust sheets of the southern Central Maine terrane sampled the deep roots of the Acadian orogen (Keller and Ague, 2018; Ferrero et al., 2021). In addition, blocks of ultrahigh-pressure rocks in the mélange indicate communication with the mantle (Keller and Ague, 2020).

The targeted hydrous ultramafic to mafic rocks constitute a near-complete cumulate line of descent formed by fractional crystallization of a hydrous parental magma at ~1,025°C and ~1.1 GPa (Tassara et al., 2021). They represent the deep subarc magmatic cumulate roots of the Acadian orogen, complementary to much of the coeval intermediate to silicic magmatism in New England (Tassara et al., 2021). They are unaltered, and only a few samples exhibit mild olivine serpentinization. The ultramafic rocks are dominantly characterized by poikilitic textures with large amphibole crystals enclosing orthopyroxene and olivine (Fig. 2A, B) or orthopyroxene crystals enclosing submillimeter cumulus olivine with variable amounts of euhedral phlogopite grains (Fig. 2C). The mafic rocks are characterized by the appearance of plagioclase in the main framework-forming mineral, with adcumulate

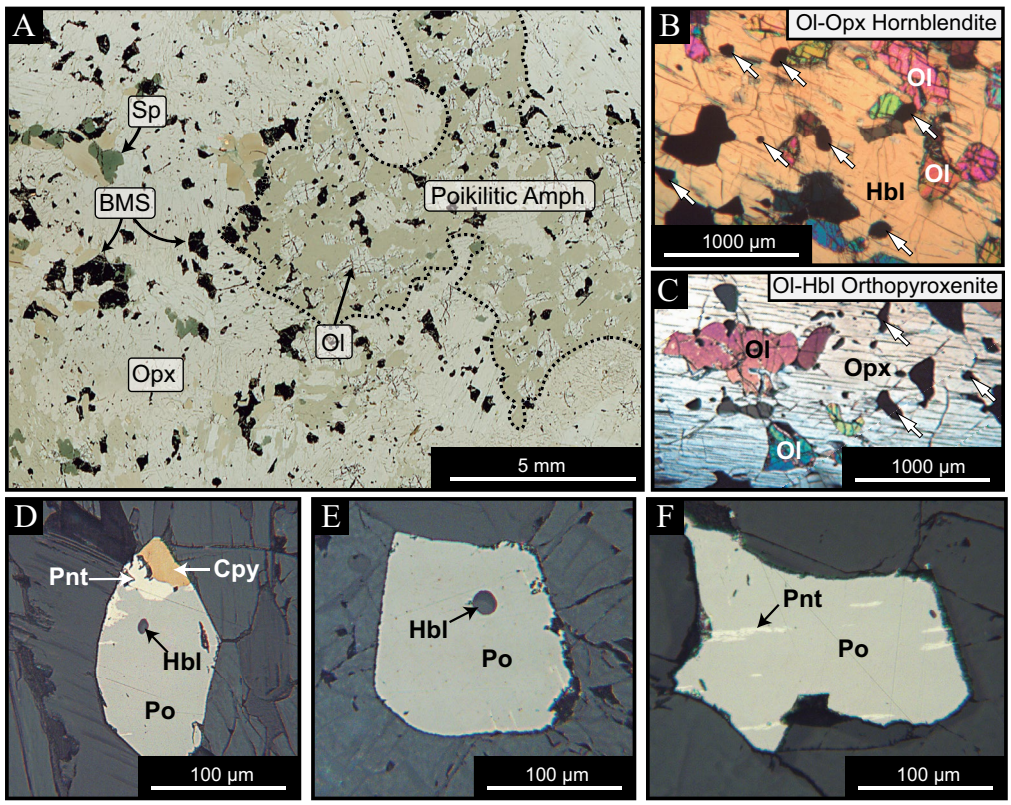

Fig. 2. Representative sulfide textures in the Acadian Cu-rich ultramafic cumulates. (A) Thin section scan of ultramafic Cu-rich cumulate showing its general appearance and the abundance and distrubition of sulfides (most of the opaque phases) in the rock. (B, C) Cross-polarized photomicrographs showing primary poikilitic textures with (B) amphibole and (C) orthopyroxene enclosing cumulus olivine and sulfide crystals. White arrows point to the location of included sulfide phases. (D-F) Reflected-light photomicrographs of individual sulfide grains. Amph = amphibole, BMS = base metal sulfide, Cpy = chalcopyrite, Hbl = hornblende, Ol = olivine, Opx = orthopyroxene, Pnt = pentlandite, Po = pyrrhotite, Sp = spinel.

amphibole. Orthopyroxene is usually large (up to 8 mm) and poikilitic and encloses euhedral phlogopite and plagioclase crystals. Accessory phases include apatite, oxides, and zircon. Oxides in the ultramafic rocks include Cr spinel, ilmenite, and minor magnetite. In the more differentiated mafic gabbros, oxides are dominantly ilmenite. Sulfide mineral abundances vary significantly. They are notably more abundant and always present in the most primitive ultramafic rocks, with a modal abundance of up to ~5%. By contrast, in the more differentiated mafic rocks, sulfides are only accessory phases. More detailed petrographic descriptions were provided by Tassara et al. (2021).

Methods

Whole-rock minor and trace elements were analyzed at the Peter Hooper GeoAnalytical Lab, Washington State University, USA. Detailed procedures can be found elsewhere (e.g., Tassara et al., 2018). The precision of the method is typically better than 5% (relative standard deviation; RSD) for the rare earth elements (REEs) and 10% for the remaining trace elements. Sulfur isotope compositions were analyzed at the Environmental Isotope Laboratory at The University of Arizona, USA. A continuous-flow isotope-ratio mass spectrometer (CF-IRMS) ThermoQuest Finnigan Delta Plus XL model coupled to a Costech elemental analyzer was used for S isotope ratio measurements. Samples were introduced into a combustion chamber with O_2 and V_2O_5 to obtain SO_2 gas at 1,300°C, which is the analyzed product. The system was calibrated using two international standards—OGS-1 and NBS123—plus several other sulfide and sulfate materials that have been compared between laboratories. The results are expressed as $\delta^{34}S$ ($\delta^{34}S = [(^{34}S/^{32}S)_{sample}/(^{34}S/^{32}S)_{CDT} - 1] \times 1{,}000$), where CDT refers to the isotopic composition of the standard Canyon Diablo Troilite. The precision (1σ) obtained for these standards is ±0.15‰. For natural samples, the precision is typically ± 0.2‰. When higher, it is due to sample heterogeneity and low S abundance.

We also determined the major element concentrations of olivine, orthopyroxene, and spinel to place constraints on oxygen fugacity. We used the JEOL JXA-8530F field emission gun (FEG) electron probe microanalyzer (EPMA) at the Yale Electron Microprobe and SEM Laboratory, Department of Earth and Planetary Sciences, Yale University. Quantitative mineral analyses were obtained using wavelength dispersive spectroscopy (WDS) using natural and synthetic standards and off-peak background corrections. Operating conditions were as follows: accelerating voltage 15 kV; beam current 15 nA; focused beam. See Ague et al. (2013) for additional information.

Results

Sulfide petrography

Sulfide phases were identified in all samples, although their nature and relative abundance vary considerably (Table 1). Individual sulfide grains range in size between ~20 and ~850 µm, with some exceptionally large and less common sulfides (>1,000 µm) in the most sulfide-rich samples (Fig. 2A-C). Sulfides are well preserved and free of alteration. They are commonly round-shaped single pyrrhotite grains or composite grains of pyrrhotite ($Fe_{0.83-1}S$) ± pentlandite ($(Fe, Ni)_9S_8$) ± chalcopyrite ($CuFeS_2$). Composite sulfide grains are characterized by a greater proportion of pyrrhotite relative to pentlandite and chalcopyrite (Fig. 2D). Whereas chalcopyrite exhibits granular forms and the contacts with pyrrhotite are sharp, pentlandite commonly displays flame-like morphologies when included in, or in contact with, pyrrhotite (Fig. 2D-F). Pentlandite and chalcopyrite typically occur on the edges of composite sulfide grains (Fig. 2D, F).

In the Cu-rich ultramafic rocks, sulfide grains are typically larger than 100 µm and can be found either included within primary silicate phases such as olivine, orthopyroxene, and amphibole (Fig. 2A-C) or along grain boundaries between silicates. Modal abundances range up to ~5% (Fig. 2A). Included sulfides may occur as single grains within olivine or orthopyroxene, or as an arrangement of abundant oikocrysts within large (>2,000 µm) poikilitic orthopyroxene or amphibole crystals. Composite sulfide grains are often texturally attached to or include micron-sized (~10–80 µm) Fe oxide phases and amphibole microcrystals (Fig. 2D, E). The abundance and nature of sulfides vary as a function of the degree of igneous differentiation as reflected by bulk-rock major element chemistry (Mg# [MgO/(MgO + FeO)] molar proportions and FeO and Al_2O_3 concentration). In agreement with the bulk-rock concentration of Cu and Ni, sulfides are more abundant in the ultramafic rocks with Mg# of ~75, and their modal proportion decreases markedly toward lower Mg#. Thus, sulfides in the more evolved mafic rocks are only accessory minerals. They are mostly pyrrhotite single grains smaller than 50 µm found within olivine and orthopyroxene crystals.

Bulk-rock lithophile elements

The major element systematics are summarized in Table 1 and plotted in Figure 3A and B. The ultramafic cumulates display a relatively narrow range of elevated Mg# (70.6–80.2) at variable SiO_2 contents (44–53.3 wt %). They have elevated FeO (up to 17 wt %) and MgO contents (up to 29 wt %), plotting close to the MgO end of the AFM diagram (A = $Na_2O + K_2O$, F = FeO_T, and M = MgO; Fig. 3B). By contrast, the mafic cumulates have a wider range of Mg# values (41.8–71.8) that decrease with decreasing SiO_2 contents (51–45.7 wt %). Their MgO contents are notably lower (5.1–13.5 wt %), extending toward the FeO end of the AFM diagram (Fig. 3B). In general, the suite of ultramafic and mafic cumulates, along with some Acadian igneous rocks in New England, display a Z-shaped pattern on an Mg# versus SiO_2 diagram, similar to cumulate suites associated with calc-alkaline magmatism elsewhere (Fig. 3A).

The trace element data are presented in Table 1, and primitive upper mantle (PUM)-normalized trace element diagrams are shown in Figure 3. The suite of ultramafic to mafic cumulates preserves most trace element indicators of subduction zone magmatism (Kelemen et al., 2007; Schmidt and Jagoutz, 2017). The rocks exhibit enrichments in large ion lithophile elements (LILEs) such as Cs, Rb, Ba, K, Pb and depletion in the high field strength elements (HFSEs) Nb, Ta, and Zr, relative to the light rare earth elements (LREEs) (Fig. 3C, D). The ultramafic rocks have elevated $(La/Yb)_N$ ratios (avg 6), moderate to high Nb/Ta (avg 12.3), and high $(U/Th)_N$ (avg 2.3), $(Ba/La)_N$ (avg 2), and $(Pb/Ce)_N$ (avg 2.4) ratios (Fig. 3C;

Table 1. Summary of Bulk-Rock and Sulfur Isotope Compositions of the Acadian Cumulates

Sample	99A	116A	160AV[1]	380	158A	117A	154A	160AC	262A	36A	78A	83B	90A	377A	64A1
Selected major elements (wt %)															
SiO_2	46.8	43.3	44.0	53.3	43.5	50.8	45.8	47.2	46.3	47.4	51.0	45.7	48.0	48.5	47.7
Al_2O_3	8.7	6.1	29.0	8.1	5.8	8.6	6.7	6.9	7.1	9.2	10.4	16.5	19.4	19.2	19.2
FeO_T	10.6	17.3	5.6	11.4	17.0	12.3	14.8	15.6	14.7	10.6	8.4	10.0	12.7	11.0	10.2
MgO	21.6	28.7	4.6	20.5	29.0	20.8	27.3	25.8	26.2	24.0	12.0	13.5	5.1	5.7	7.3
Mg#	78.5	74.8	59.3	76.2	75.2	75.0	76.8	74.7	76.1	80.2	71.8	70.6	41.8	47.9	56.2
Minor and trace elements (μg.g^{-1})															
Ni	381	1,358	743	639	1,595	1,033	1,700	1,683	1,466	715	70	350	7	12	33
Cr	1,573	706	14	682	700	1,181	840	657	577	1,654	564	563	bdl	bdl	10
V	175	53	10	164	54	216	98	58	80	184	241	169	526	414	429
Cu	141	511	296	81	692	246	728	664	461	39	57	30	117	34	48
Zn	82.1	182.1	14.8	85.7	170.6	84.5	73.1	78.8	67.4	76.5	61.8	188.3	143.5	82.6	80.3
Cs	5.2	1.2	0.2	1.2	1.0	1.3	3.1	5.0	2.3	1.3	1.1	1.2	1.0	1.0	2.4
Rb	145.6	14.6	5.8	53.7	11.6	32.0	42.5	62.9	23.9	20.7	45.1	56.0	54.3	52.3	63.0
Ba	306	83	86	91	73	89	111	326	105	203	318	268	475	416	538
Th	1.9	1.4	12.1	1.2	1.3	1.5	1.6	1.3	2.3	3.0	2.0	0.8	1.4	1.6	1.0
U	0.6	0.6	14.7	0.6	0.5	1.3	1.2	1.1	0.7	0.7	0.8	0.3	1.2	1.5	1.8
Ta	0.4	0.2	0.4	0.5	0.2	0.3	0.2	0.4	0.3	0.2	0.2	0.2	0.8	0.4	1.8
Nb	6.8	2.5	1.8	6.5	2.4	3.6	3.0	3.8	3.1	3.2	3.8	2.6	8.3	5.2	8.0
La	17.9	6.3	18.7	4.1	5.9	8.1	9.4	4.2	8.3	10.2	14.4	6.0	5.8	7.6	7.3
Ce	45.4	12.7	20.9	12.5	12.5	20.7	26.1	8.6	15.9	20.5	33.1	13.5	16.7	18.9	18.4
Pb	1.2	1.1	15.0	3.2	1.9	2.0	3.0	2.9	2.9	4.3	4.7	10.2	10.3	9.6	9.6
Pr	6.3	1.5	2.0	2.0	1.5	2.9	3.6	1.1	1.8	2.6	4.4	1.9	2.8	2.8	2.7
Sr	64	89	3,526	56	83	79	67	86	125	236	317	362	252	308	259
Nd	25.9	6.2	6.9	9.8	6.2	12.5	15.2	4.4	6.9	10.9	19.2	8.3	14.6	14.1	12.8
Hf	3.0	1.3	2.4	1.7	1.2	1.8	1.4	1.3	1.7	1.7	2.6	1.7	2.1	1.5	1.6
Zr	119	58.6	73	66.5	48.9	72.9	48.4	52.7	69.6	55.8	84.3	65.2	59.2	34.8	44.2
Sm	5.6	1.5	1.5	3.1	1.4	2.9	3.5	1.1	1.6	2.8	4.8	2.4	5.3	4.5	4.1
Eu	1.1	0.5	1.3	0.6	0.5	0.7	0.7	0.3	0.5	0.7	1.5	0.9	1.4	1.4	1.3
Gd	5.3	1.5	1.4	3.4	1.5	2.8	3.2	1.2	1.6	2.9	4.7	2.7	6.4	5.4	5.1
Tb	0.8	0.3	0.3	0.6	0.2	0.5	0.5	0.2	0.3	0.4	0.8	0.5	1.3	1.0	1.0
Dy	5.0	1.5	1.6	3.3	1.5	2.9	3.1	1.5	1.8	2.9	4.5	2.9	8.4	6.3	6.4
Y	24.5	8.1	9.4	15.6	8.0	14.3	15.5	7.8	9.2	14.3	21.1	15.3	47.2	33.9	35.0
Ho	0.9	0.3	0.3	0.6	0.3	0.6	0.6	0.3	0.3	0.6	0.9	0.6	1.8	1.3	1.4
Er	2.5	0.8	0.8	1.6	0.8	1.5	1.6	0.8	1.0	1.5	2.2	1.6	5.1	3.6	3.8
Tm	0.4	0.1	0.1	0.2	0.1	0.2	0.2	0.1	0.1	0.2	0.3	0.2	0.8	0.5	0.6
Yb	2.2	0.8	0.8	1.4	0.8	1.3	1.3	0.7	0.9	1.3	1.8	1.4	5.1	3.3	3.5
Lu	0.3	0.1	0.1	0.2	0.1	0.2	0.2	0.1	0.1	0.2	0.3	0.2	0.8	0.5	0.5
Sulfide abundance	xx	xxx	xx	xx	xxxx	xxx	xxxx	xxxx	xxxx	x	x	x	xx	x	x
Sulfur isotopes (‰)															
$\delta^{34}S$	–4.9	–3.2	–3.2	–3.1	–3	–2.9	–2.90	–2.9	–2.2	–1.2	–0.6	3.8	4.3	5.6	8
$\pm\delta^{34}S$ (1σ, n = 3)	0.86	0.15	0.15	0.86	0.15	0.24	0.15	0.15	0.15	0.86	0.24	0.86	0.24	0.86	0.86

FeO_T is total iron expressed as FeO; major element data are from Tassara et al. (2021); number of *X*s represents relative abundance of sulfide phases in the rocks

σ = standard deviation, bdl = below detection limit

[1]Sample 160AV corresponds to a plagioclase-rich vein crosscutting ultramafic lithologies

Table 1). In the ultramafic rocks, LILE enrichment is controlled by the abundance of amphibole and phlogopite. Some phlogopite-rich samples have low Sr/Nd and Pb/Ce anomalies. The mafic gabbronorites exhibit LILE enrichment and Nb and Ta depletions comparable to the ultramafic rocks but also stronger Zr and Hf depletions and variably lower $(La/Yb)_N$ ratios between 0.8 and 7.6 (Fig. 3D).

Bulk-rock copper and nickel

The concentrations of Cu and Ni in the ultramafic and mafic cumulates are listed in Table 1 and plotted in Figure 4. The concentrations of Cu and Ni are highly correlated throughout the entire suite (Fig. 4A). The concentration of Cu ranges from 30 to 728.2 μg g^{-1}, and the concentration of Ni ranges from 7 to 1,700 μg g^{-1}. Copper concentrations are directly correlated with FeO (R^2 = 0.86) (Fig. 4B) and are relatively low in the cumulate rocks with Mg# < 74 (30–117.5 μg g^{-1}). However, they increase markedly at Mg# > 74, reaching maximum values up to 728.2 μg g^{-1} (Fig. 4C).

Bulk-rock sulfur isotope compositions

A total of 15 cumulates were analyzed for their bulk-rock S isotope compositions (Table 1; Fig. 5). Sulfur isotope compositions range between $\delta^{34}S$ –4.9 and 8‰. The Cu, Ni, and sulfide-rich ultramafic rocks always display negative values (–4.9 to –1.2‰), averaging –3‰. In contrast, the most differentiated mafic rocks depleted in Cu and Ni have dominantly positive $\delta^{34}S$ values ranging between –0.6 and 8‰ (Fig. 5).

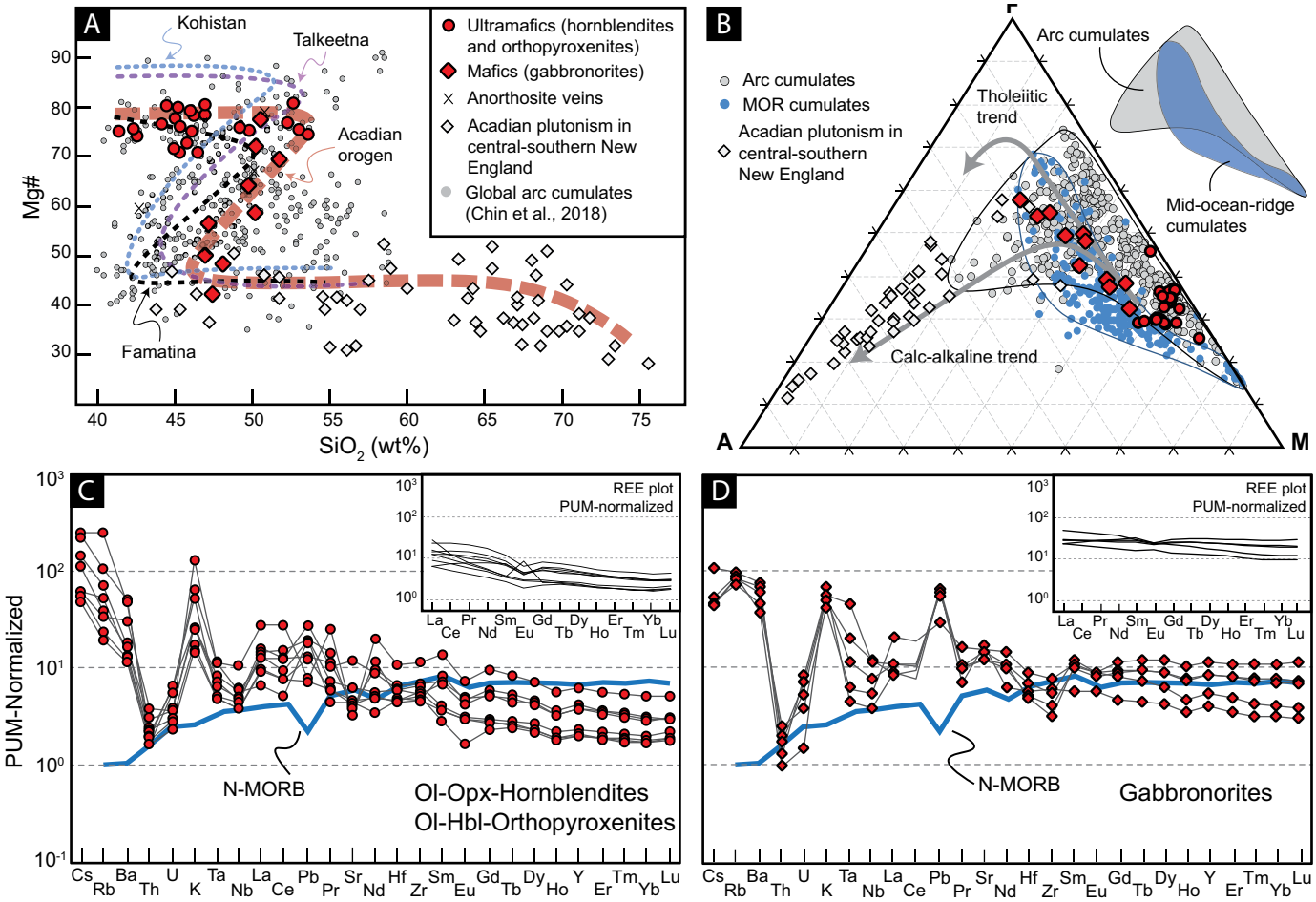

Fig. 3. Bulk-rock major and trace element composition of the Acadian cumulate rocks. (A) Mg# [Mg# = 100 × MgO/(MgO + FeO) molar proportions] plotted against SiO_2. (B) AFM (A = Na_2O + K_2O, F = FeO_T, and M = MgO) diagram showing the composition of Acadian cumulates and coeval evolved magmatism in New England. Fields for mid-ocean ridge (MOR) and subarc cumulates after Chin et al. (2018). (C, D) Primitive upper mantle (PUM)-normalized trace element patterns for ultramafic (C) and mafic (D) Acadian cumulates. Mid-ocean ridge basalt (MORB) composition after McDonough and Sun (1995). Hbl = hornblende, N-MORB = normal mid-ocean ridge basalt, Ol = olivine, Opx = orthopyroxene, REE = rare earth element.

The bulk $\delta^{34}S$ of the rock suite correlates well with indices of magmatic differentiation, such as the Mg# (R^2 = 0.71), MgO (R^2 = 0.75), and Al_2O_3 (R^2 = 0.9) contents (Fig. 5). In addition, we analyzed the S isotope composition of associated metasedimentary rocks exposed by the same thrust sheets. Results indicate strongly negative $\delta^{34}S$ values ranging from –19.5 to –12‰ (Table 2).

Mineral compositions

Olivine, orthopyroxene, and spinel crystals were analyzed in three different samples (JAQ36, JAQ158, and JAQ116) for their major element chemistry. The compositions are summarized in Table 3, where each row represents the average of two to four crystal cores. Forsterite contents in cumulus olivine range from 78 to 81, with the least refractory olivines displaying higher MnO and NiO concentrations (sample JAQ36). Intercumulus orthopyroxene grains are magnesian (Mg# 80–82), have low CaO (<0.3 wt %), and have variable Al_2O_3 (1.81–3 wt %). Granular, green spinel is rich in hercynite, with Al_2O_3 concentrations that range from 57.1 to 61.1 wt %. The MgO content in spinel varies from 13.6 to 16.6 wt %, and Cr_2O_3 concentrations can be as much as 7.6 wt %.

Archive of Subduction Zone Signatures in Subarc Cumulates

Several lines of evidence indicate that the rock suite studied herein represents the deep subarc hydrous cumulate roots of the Acadian orogen:

1. Thermobarometric estimates obtained via two-pyroxene thermobarometry (Putirka, 2008, their eq. 38) and amphibole chemistry (Al-in-hornblende; following Larocque and Canil, 2010) suggest crystallization conditions of ~1,000°C and ~1.1 GPa, indicating depths of 40–45 km based on lithostatic pressure (Tassara et al., 2021). These pressure and temperature conditions are consistent with those of surrounding ultrahigh-temperature metamorphic rocks (>1 GPa; Ague et al., 2013).
2. The typical orthocumulate to adcumulate textures and the elevated Mg# and mean FeO (~11 wt %) and TiO_2

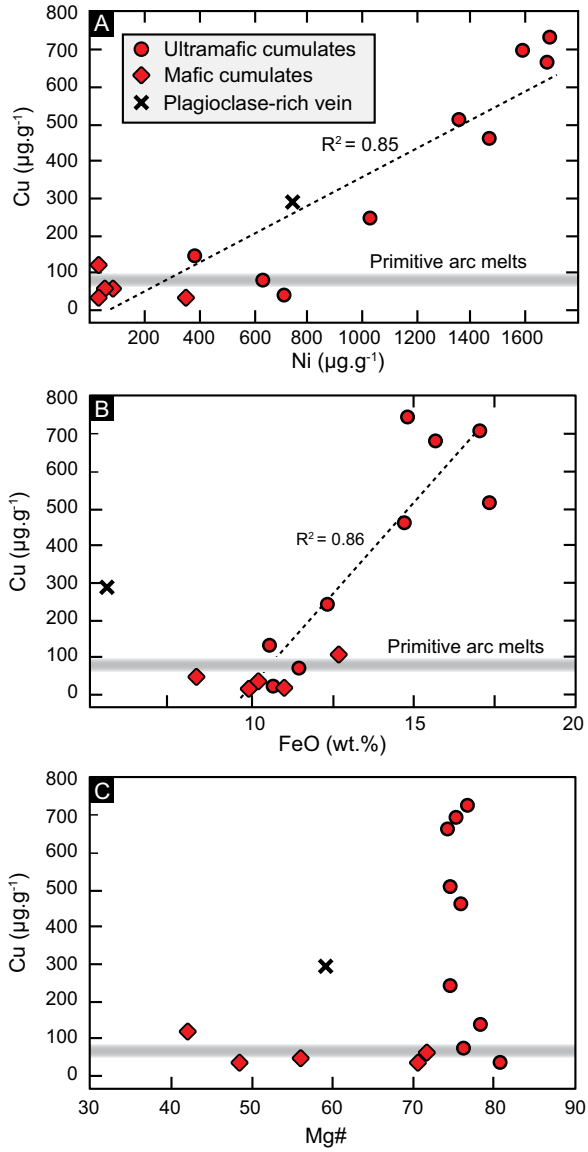

Fig. 4. Copper concentration in the Acadian cumulates plotted against Ni (A), FeO (B), and Mg# (C). The primitive arc magmas Cu content is after Lee et al. (2012).

(~0.85 wt %) contents are consistent with the composition of hydrous cumulates formed formed during fractionation of calc-alkaline magmas in continental arcs (Fig. 3B; Chin et al., 2018).

3. The Z-shaped pattern defined by the major element systematics in the Mg# versus SiO_2 space (Fig. 3A) is due to the cumulate line of descent that results from the fractionation of hydrous basaltic to andesitic melts at high pressure (>0.7 GPa; Jagoutz et al., 2011; Walker et al., 2015; Müntener and Ulmer, 2018; Tassara et al., 2021). In addition, the age (~410 Ma) and trace element systematics (Dy/Yb) suggest that these subarc hydrous cumulates are complementary magmatic residues to much of the evolved coeval plutonism in the New England Appalachians (Tassara et al., 2021).

In addition to their major element composition, the bulk-rock trace element data also document characteristic features of hydrous calc-alkaline arc magmas, including high ratios of light to heavy REEs (LREE/HREE), enrichment in LILEs, and depletion in the fluid immobile elements Nb and Ta compared to LREEs (Fig. 3; Kelemen et al., 2007; Schmidt and Jagoutz, 2017). Although these rocks have a cumulate origin and their bulk chemistry does not reflect that of a true melt, it is well established that cumulate rocks can inherit and record most trace element signatures from their parental melts depending on the abundance of trapped intercumulus liquid (Barnes, 1986; Cawthorn, 1996). In the present case, the most primitive ultramafic orthocumulates have significant amphibole as oikocrysts distributed among the early formed cumulus minerals (olivine, spinel, orthopyroxene), which indicates the presence of intercumulus melt during crystallization (Smith, 2014; Chang and Audétat, 2018). The amount of crystallized intercumulus melt decreases in the most differentiated gabbroic rocks with mesocumulate textures. Thus, the overall trace element systematics of the studied rocks support the interpretation that they are arc-related cumulates formed after hydrous calc-alkaline parental magmas (Fig. 3).

Sulfides: A Primary or Secondary Origin?

Base metal sulfides are ubiquitous phases in ultramafic and mafic rocks from the lower crust and mantle lithosphere. However, in addition to a primary magmatic origin, late-stage alteration of slowly cooled and exhumed ultramafic rocks can result in the formation of secondary sulfide mineral assemblages. Secondary processes include the removal, modification, or formation of hydrothermal sulfides due to open-system fluid-rock interaction during exhumation or weathering.

The sulfides of the studied rocks are single pyrrhotite grains or composite grains of pyrrhotite ± pentlandite ± chalcopyrite (Fig. 2). These assemblages typically form during subsolidus reequilibration of initially crystallized monosulfide solid solution (MSS) (Ballhaus et al., 2001). The flame-like texture of pentlandite within pyrrhotite grains supports this interpretation (Fig. 2E). In addition, the sulfides dominantly occur within magmatic silicate phases (olivine, orthopyroxene, amphibole), distal to visible cracks or fractures, and sometimes even include micron-sized amphibole crystals (Fig. 2D). In agreement with the fresh and unaltered nature of the samples, these observations indicate that the sulfide assemblages of the Acadian subarc cumulates have a primary magmatic origin.

Hydrous Subarc Cumulates as a Sink for Copper during Arc Magmatism

The formation of subarc Cu-rich cumulates during the geochemical differentiation of arc magmas has been largely inferred from the study of eruptive volcanic products (Jenner et al., 2010; Lee et al., 2012; Chiaradia, 2014). By contrast, direct evidence for Cu enrichment in the complementary subarc cumulates remains meager, in part because of the inherently limited access to the deepest roots of arcs. However, examples of Cu enrichment (>500 µg g^{-1}) in subarc cumulates have been provided for garnet-pyroxenite xenoliths from Sierra Nevada and Arizona (Lee et al., 2012; Chen et al., 2020), as well as a few exhumed amphibole gabbronorites from the Talkeetna arc crustal section in Alaska (Greene et al., 2006). The existence of garnet-bearing Cu-rich cumulates

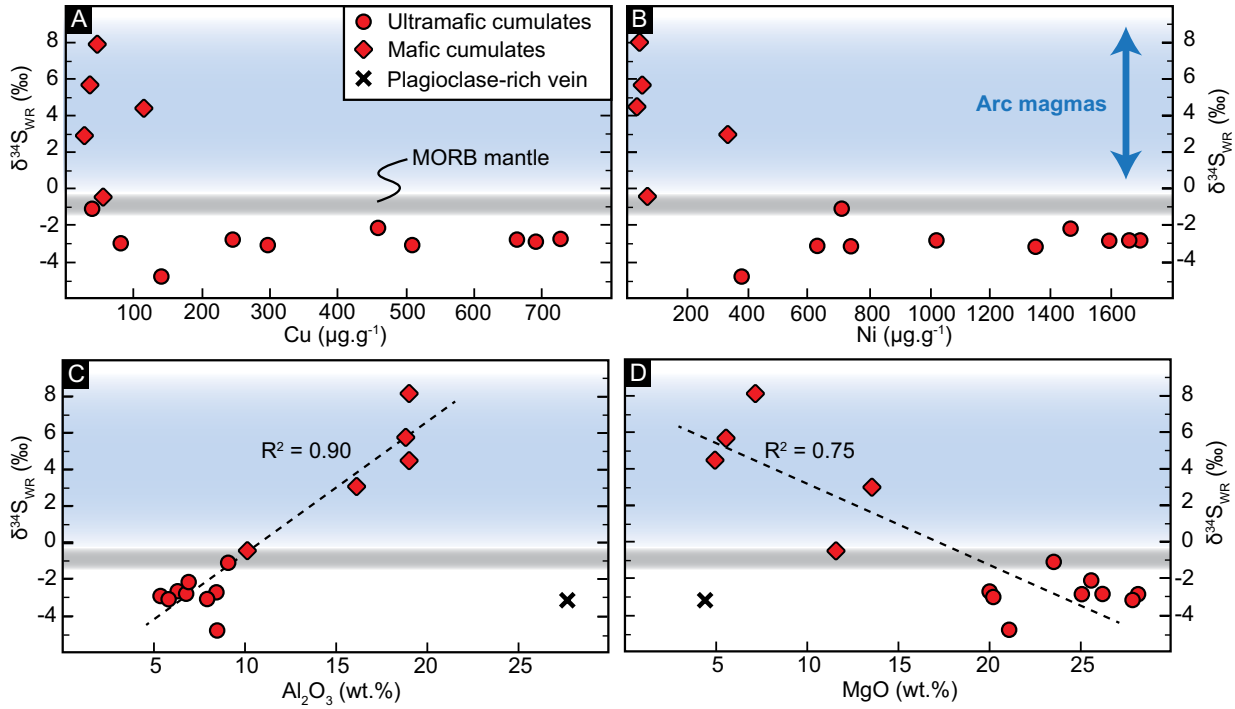

Fig. 5. Sulfur isotope systematics of the Acadian cumulates plotted against (A) Cu, (B) Ni, (C) Al_2O_3, and (D) MgO. Gray bar indicates estimates of mid-ocean ridge basalt (MORB) mantle source S isotope composition after Labidi et al. (2012). Light-blue gradient indicates the range of S isotope composition for arc magmas worldwide (Muth and Wallace, 2021). Panels C and D exclude the plagioclase-rich vein from the linear regression. WR= whole rock.

is consistent with the interpretation that the overriding plate thickness in subduction zones plays a crucial role in the Cu concentration of arc magmas (Chiaradia, 2014), as garnet may be an early-crystallized phase at pressures above ~1.2 GPa and hydrous (~4 wt % H_2O) conditions (Müntener et al., 2001; Müntener and Ulmer, 2018). However, Cu seems to behave compatibly during magmatic differentiation in arcs with crusts of 30–45 km (Chiaradia, 2014; Jenner, 2017), where lithostatic pressure is insufficient to stabilize garnet in hydrous basalts, and amphibole dominates instead (Alonso-Perez et al., 2009). Indeed, whereas the observed phase assemblages in natural subarc cumulate rocks vary widely, many examples formed at pressures below the garnet stability field and are dominated by amphibole (e.g., Behn and Kelemen, 2006; Jagoutz and Behn, 2013; Velazquez Santana et al., 2020). Importantly, amphibole fractionation is being increasingly recognized in the differentiation of arc magmas (e.g., Davidson et al., 2007; Alonso-Perez et al., 2009; Larocque and Canil, 2010; Dessimoz et al., 2012; Bucholz et al., 2014; Walker et al., 2015; Du and Audétat, 2020; Zhou et al., 2020; Barber et al., 2021; Tassara et al., 2021). Our data provide direct evidence for Cu enrichment (up to ~730 µg g^{-1}) in amphibole-dominated subarc cumulates during the construction of the Appalachians (Fig. 4). In addition, the Cu content of the Acadian subarc cumulates is highest in the most primitive and FeO-richest samples (~17.3 wt %) and decreases with decreasing FeO (R^2 = 0.86) (Fig. 4B). This correlation indicates that the processes driving the petrogenetic evolution of the parental magmas may have also exerted a primary control on sulfide saturation. Thus, our data show that amphibole (± Fe-Ti oxide)-dominated subarc cumulates can be important sinks for Cu during the early geochemical differentiation of calc-alkaline arc magmas.

Table 2. Sulfur Isotope Composition of Associated Graphite-Bearing Metasedimentary Rocks

Sample	Comment	$\delta^{34}S$ (‰)	$\pm\delta^{34}S$ (1σ, n = 3; ‰)
20161118	Visible sulfide	–19.47	0.15
QP-1	Visible sulfide	–12.14	0.15
JAQ60A	Widespread sulfide	–18.60	0.15
JAQ221A	Rich in disseminated sulfide	–16.07	0.15
JAQ324A	Visible sulfide	–18.64	0.15
JAQ335A	Disseminated sulfides	–15.12	0.15
JAQ366A	Disseminated sulfides	–15.62	0.15

Most sulfide in the analyzed metasedimentary rocks is pyrrhotite

The Nature of Sulfur Locked in Subarc Cumulates

Sulfur isotopes as archives of deep petrogenetic processes

In addition to the S isotope composition of the source of magmas, S degassing, fractional crystallization, and assimilation of crustal material during ascent throughout the crust can control the $\delta^{34}S$ signature of igneous rocks (Marini et al., 2011). Because ^{34}S is preferentially retained in oxidized S species, degassing of SO_2 from oxidized melts (where S is dominantly dissolved as S^{6+}) can lead to increasing melt $\delta^{34}S$, and degassing of H_2S from reduced melts (where S is dominantly dissolved as S^{2-}) can lead to decreasing melt $\delta^{34}S$ (Ohmoto and Rye, 1979; Fiege et al., 2014). However, the elevated pressures at which the studied ultramafic rocks crystallized (~1.1 GPa) in the lower crust and the consequently increased water solubility

Table 3. Oxides for Minerals Used for Oxybarometric Estimates (wt %)

Mineral	ID	SiO_2	TiO_2	Al_2O_3	Cr_2O_3	MgO	FeO	NiO	ZnO	MnO	CaO	Na_2O	K_2O	Total	fo_2 (ΔFMQ)
Sp	JAQ36av1	0.04	bdl	58.21	5.79	14.04	20.90	0.23	1.61	0.15	bdl	bdl	bdl	100.95	
Opx	JAQ36av1	54.35	0.05	3.01	0.16	28.97	13.20	0.03	0.00	0.25	0.10	bdl	bdl	100.14	–1.93
Ol	JAQ36av1	39.34	bdl	bdl	bdl	40.34	20.39	0.17	bdl	0.24	bdl	bdl	bdl	100.50	
Sp	JAQ36av2	0.04	bdl	58.32	5.67	14.06	20.87	0.18	1.71	0.18	bdl	bdl	bdl	101.03	
Opx	JAQ36av2	55.09	0.04	1.81	0.09	29.17	13.64	0.02	0.01	0.27	0.12	bdl	bdl	100.23	–1.79
Ol	JAQ36av2	39.52	bdl	bdl	bdl	40.86	20.43	0.19	bdl	0.22	bdl	bdl	bdl	101.23	
Sp	JAQ36av3	0.03	bdl	57.12	7.58	13.56	21.59	0.20	1.17	0.22	bdl	bdl	bdl	101.47	
Opx	JAQ36av	54.98	0.05	2.31	0.11	29.39	13.11	0.03	0.02	0.25	0.08	bdl	bdl	100.34	–2.21
Ol	JAQ36av3	39.30	bdl	bdl	bdl	40.65	20.63	0.19	bdl	0.23	bdl	bdl	bdl	101.00	
Sp	JAQ158av1	0.03	0.10	61.10	2.30	15.70	17.00	bdl	1.70	0.10	bdl	bdl	bdl	98.03	
Opx	JAQ158av2	54.70	0.07	2.39	0.17	30.30	11.50	bdl	bdl	bdl	0.30	bdl	bdl	99.43	–2.34
Ol	JAQ158av1	39.15	bdl	bdl	bdl	42.70	17.90	bdl	bdl	0.20	bdl	bdl	bdl	99.95	
Sp	JAQ158av2	0.07	0.10	59.43	4.11	15.13	17.30	bdl	1.50	0.13	bdl	bdl	bdl	97.77	
Opx	JAQ158av1	54.50	0.10	2.39	0.18	30.25	11.50	bdl	bdl	bdl	0.30	0.01	bdl	99.23	–2.51
Ol	JAQ158av2	39.13	bdl	bdl	0.02	42.73	17.63	bdl	bdl	0.17	bdl	bdl	bdl	99.69	
Sp	JAQ116av1	0.10	bdl	58.20	5.85	16.40	17.00	bdl	0.58	0.10	bdl	bdl	bdl	98.23	
Opx	JAQ116av1	54.30	0.10	2.83	0.04	29.95	11.50	bdl	bdl	0.20	bdl	bdl	bdl	98.91	–2.22
Ol	JAQ116av1	38.97	bdl	bdl	0.02	42.47	17.30	bdl	bdl	0.17	bdl	bdl	bdl	98.92	
Sp	JAQ116av2	0.10	0.10	61.00	1.95	16.60	16.50	0.10	1.15	0.10	bdl	bdl	bdl	97.60	
Opx	JAQ116av2	53.75	0.10	2.93	0.07	30.05	11.50	bdl	bdl	0.20	bdl	bdl	bdl	98.59	–2.14
Ol	JAQ116av2	38.65	bdl	bdl	0.02	42.40	17.65	bdl	bdl	0.15	bdl	bdl	bdl	98.87	

Each composition represents the average of two to four analyzed crystal cores
bdl = below detection limit, FMQ = fayalite-quartz-magnetite buffer, Ol = olivine, Opx = orthopyroxene, Sp = spinel

minimize the potential effects of degassing on their S isotope composition. Furthermore, if significant S degassing occurred at depth, it should have kept the parental magma at sulfide-undersaturated conditions, which is clearly not the case (Fig. 2). In contrast, given their cumulate nature, fractional crystallization is obviously a critical process in our suite of rocks.

To test the effects of fractional crystallization on the $\delta^{34}S$ values, we modeled the S isotope evolution of mantle-derived parental melts via Rayleigh fractionation. This scenario illustrates the most extreme form of fractionation. The equations describing the evolution of the melt and corresponding cumulate are well established (Criss, 1999):

$$\delta^{34}S_{melt} = \delta^{34}S_{source} + 1{,}000 \times \left(F^{(\alpha_{silicate-sulfide}-1)} - 1\right) \quad (1)$$

$$\delta^{34}S_{cumulate} = \delta^{34}S_{source} + 1{,}000 \times \alpha_{silicate-sulfide} \times \left(F^{(\alpha_{silicate-sulfide}-1)} - 1\right), \quad (2)$$

where $\delta^{34}S_{source}$ is the initial $\delta^{34}S$ value of the parental melt, F is the fraction of S remaining in the melt, and $\alpha_{silicate\text{-}sulfide}$ is S isotope fractionation factor between silicate melts and sulfides. Initial source $\delta^{34}S_{source}$ values were assumed to be mantle-like (5.5‰; Labidi et al., 2012). At the elevated temperatures at which the cumulates formed (~1,025°C; Tassara et al., 2021), the $\alpha_{silicate\text{-}sulfide}$ is 1.0000 ± 0.0005 (Mandeville et al., 2009; Labidi and Cartigny, 2016). This model predicts that the isotopic fractionation can only change by ~2‰ after the removal of nearly all of the S initially present in the melt, which is unlikely. The model also shows that the $\delta^{34}S$ composition of the complementary cumulate follows that of the evolving melt at ±0.5‰.

The above discussion indicates that neither S degassing nor sulfide fractionation can account for the full range of S isotope variations observed in the subarc cumulates (Fig. 5). Therefore, the measured $\delta^{34}S$ must reflect deep-seated petrogenetic processes; the observed correlations between $\delta^{34}S$ and Al_2O_3 (positive, $R^2 = 0.90$), MgO (negative, $R^2 = 0.75$), and Mg# (negative, $R^2 = 0.71$) are most likely explained by the assimilation of S-bearing material (Fig. 5C, D). In situ zircon Hf isotope systematics provide a key test of this hypothesis and show that the parental magmas to the ultramafic Acadian cumulates underwent crustal assimilation during their petrogenetic evolution (Tassara et al., 2021). Possible assimilated lithologies in the Acadian orogen include preexisting metasedimentary rocks accreted to the base of the crust during the protracted history of collision and terrane accretion in the New England Appalachians. Such underthrusted rocks have been recognized as important components during arc magmatism in the Acadian orogen and elsewhere (DeCelles et al., 2009; van Staal et al., 2009; Li, J.Y., et al., 2021). Similar lithologies have been shown to be buried to at least 60-km depth (Keller and Ague, 2018, 2020; Ferrero et al., 2021), leading to a scenario of potential deep melt-sediment interaction in the lower crust.

The origin of light S isotope signatures in the most primitive Acadian cumulates

The most primitive ultramafic subarc cumulates analyzed herein have an average $\delta^{34}S$ of –3‰. However, typical primitive arc magmas generally have relatively heavy S isotope signatures ($\delta^{34}S$ up to ~10‰; Alt et al., 1993; Metrich et al., 1999;

de Hoog et al., 2001; Wallace and Edmonds, 2011; Muth and Wallace, 2021). In addition, mid-ocean ridge basalts have a $\delta^{34}S$ composition of –0.91 ± 0.50‰ (Labidi et al., 2012). As such, the relatively light –3‰ values observed in the most primitive Acadian subarc cumulates require an alternative source of isotopically light S to the parental mantle magmas. Two main mechanisms can explain their $\delta^{34}S$ composition. The first possibility is that assimilation of isotopically light S-bearing crustal material occurred early during the evolution of parental magmas to the Acadian cumulates. An alternative possibility is that their parental magmas formed from a mantle source metasomatized by isotopically light slab-derived fluids. Recent studies have shown that the dehydration of slab components can release fluids with a range of light to heavy S isotope compositions ($\delta^{34}S$ between –11 and 8‰) beneath the arc window (Bénard et al., 2018; Walters et al., 2019; Li, J.L., et al., 2020, 2021). Thus, mixing of isotopically light S-bearing slab fluids with a peridotite mantle source could result in primitive parental magmas with $\delta^{34}S$ signatures of –3‰.

However, we favor an assimilation-driven scenario because (1) most primitive arc melts display isotopically heavy S isotope compositions (Alt et al., 1993; Metrich et al., 1999; de Hoog et al., 2001; Wallace and Edmonds, 2011; Muth and Wallace, 2021); (2) a crustal component is nearly ubiquitous in the Acadian magmatism as well as in other accretionary orogens elsewhere where crustal thickening increases the degree to which ascending mantle-derived magmas interact with crustal material (DePaolo, 1981; Ague and Brimhall, 1987, 1988; Hildreth and Moorbath, 1988; Dorais, 2003; Annen et al., 2006; DeCelles et al., 2009; Walker et al., 2015); (3) the ultramafic cumulates are emplaced within a lower crust rich in isotopically light sulfidic metasedimentary material (Table 2); (4) in situ zircon Hf isotope data show that the parental magmas to the ultramafic cumulates assimilated crustal material (Tassara et al., 2021); and (5) assimilation of metasedimentary crust is consistent with the elevated modal abundance of orthopyroxene (because of higher silica activity) and phlogopite (source of K) in the primitive Acadian cumulates. To test this interpretation, we analyzed the S isotope composition of sulfidic (and graphite-rich) high-pressure and high-temperature metasedimentary rocks associated with the ultramafic cumulates in the exposed mélange complex. Results show that these rocks have $\delta^{34}S$ between –19.5 and –12‰ (Table 2). A simple mixing model assuming an parental magma with $\delta^{34}S$ of ~6‰ shows that a mass fraction of ~5–35% of assimilated material relative to the parental magmas can account for the observed $\delta^{34}S$ –3‰ signature of the parental magmas to the Acadian subarc cumulates (the higher the S concentration in the assimilant, the lower the required mass; Fig. 6). Our interpretation can be further tested in the future using additional isotopic studies including oxygen and osmium, both of which have been shown to be highly sensitive to assimilation processes (e.g., Taylor, 1980; Taylor and Sheppard, 1986; Saal et al., 1998).

Systematics of sulfur in the more evolved Acadian cumulates

Our data show that whereas the most primitive parental magmas to the cumulates had a light S isotope composition ($\delta^{34}S$ –3‰), the more evolved cumulates display isotopically heavy S isotope compositions (up to $\delta^{34}S$ 8‰; Fig. 5). These results are comparable to those obtained for the Sierra Nevada

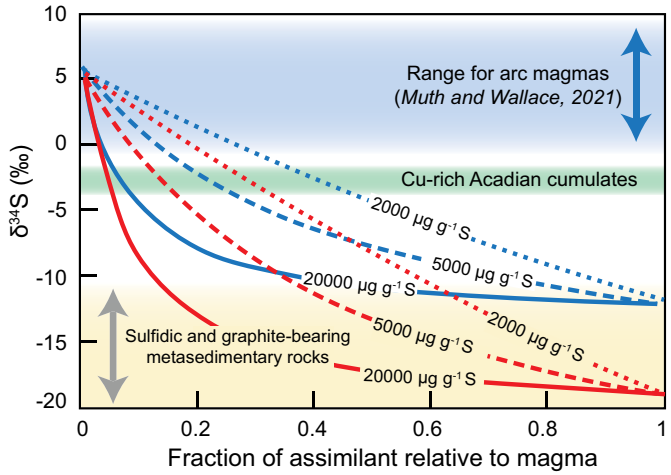

Fig. 6. Isotopic result of mixing between typical arc magmas and metasedimentary crustal material in the Acadian orogen. The initial $\delta^{34}S$ composition of the magma is 5.5‰ with 1,500 µg g^{-1} S. Blue lines represent mixing with crustal material with a $\delta^{34}S$ of –12‰. Red lines represent mixing with crustal material with a $\delta^{34}S$ of –19.5‰. Each line denotes variable S concentrations in the assimilated rocks.

subarc garnet-bearing cumulates, which show a variation of ~6‰ in their $\delta^{34}S$ signatures from mantle-like values in the direction of seawater (Lee et al., 2018). In this case, the shift was interpreted to be the result of assimilation of isotopically heavy S during differentiation. Although modern marine sedimentary sulfides that formed by bacterial reduction exhibit dominantly light $\delta^{34}S$ values, early Paleozoic and late Proterozoic sedimentary sulfides worldwide have a wide range of isotopic compositions, from strongly negative to strongly positive values (approximately from –30 to 40‰; Rickard, 2014). Therefore, it may be possible that the $\delta^{34}S$ of composition of the more evolved Acadian cumulates reflects the assimilation of isotopically heavy crustal material. However, there is currently neither field evidence for isotopically heavy material that could be potentially assimilated nor independent geochemical data that support such an interpretation. By contrast, because the $\delta^{34}S$ composition of the more evolved Acadian cumulates is comparable to the range of $\delta^{34}S$ values of primitive arc magmas globally (Alt et al., 1993; de Hoog et al., 2001; Wallace and Edmonds, 2011; Muth and Wallace, 2021), the Acadian gabbros may simply reflect the composition of a parental primitive magmas with isotopically heavy S that experienced little to no assimilation of crustal material. In this scenario, the Acadian gabbros and ultramafic cumulates may have formed from different batches of similar magmas that originally had relatively heavy S isotope signatures (e.g., 6–8‰ $\delta^{34}S$). As such, the assimilation of variable amounts of isotopically very light S-bearing crustal material can fully explain the observed variation of $\delta^{34}S$ values.

Sulfide Saturation Caused by Crustal Assimilation

We have provided petrographic and geochemical evidence for the presence of deep-seated Cu-rich amphibole-dominated cumulates at the base of the Acadian orogen (~40–45 km; Tassara et al., 2021). In this section, we address the mechanisms responsible for their formation. At the high pressures at which magmas pond and fractionate at the base of continental

arcs, the stability of sulfide phases expands toward higher f_{O_2} values (Matjuschkin et al., 2016). Therefore, most arc magmas are likely to undergo some degree of sulfide saturation during their early geochemical evolution (Lee et al., 2012; Jenner, 2017). However, it has become evident that not all subarc cumulates display particularly elevated Cu contents (Rezeau and Jagoutz, 2020). Instead, the Cu content of the fractionated cumulates will likely depend on the efficiency of sulfide accumulation and the degree to which the parental magmas undergo sulfide saturation. The high Cu contents and elevated sulfide modal proportions of the Acadian ultramafic cumulates clearly indicate significant sulfide saturation in their parental magmas. In addition, field relationships and the S isotope composition of the most primitive—and Cu-rich—Acadian cumulates are consistent with the assimilation of graphite-bearing sulfidic metasedimentary crustal material. These observations suggest a link between crustal assimilation during magmatic differentiation, sulfide saturation, and the consequent formation of Cu-rich subarc cumulates.

The assimilation of preexisting crustal material by ascending arc magmas has the potential to drive significant changes in three of the fundamental parameters that control S solubility. First, crustal assimilation typically causes a decrease in FeO and an increase in SiO_2 concentrations because the lowest melting fraction of most preexisting crustal material is generally of felsic composition (Phillipots and Ague, 2009). Secondly, the latent heat of fusion required to melt and assimilate crustal material consumes vast quantities of energy, resulting in a temperature decrease of the evolving magma (DePaolo, 1981). Third, crustal assimilation can induce oxidation or reduction of magmas—or result in no f_{O_2} change—depending on the nature of the assimilated material (e.g., Ague and Brimhall, 1987, 1988; Grocke et al., 2016). Specifically, assimilation of reducing graphitic metasedimentary crust leads to a significant decreae of the f_{O_2} of the evolving magma (Ague and Brimhall, 1987; Tomkins et al., 2012). Thus, all of the above-mentioned consequences of crustal assimilation can ultimately lead to decreases in S solubility that would be expected to promote sulfide saturation.

The effects of crustal assimilation on sulfide saturation are best illustrated in view of genetic models for the formation of magmatic sulfide ore deposits. Amphibole and orthopyroxene rich lithologies—such as the Cu-rich Acadian cumulates studied herein and some Cu-rich amphibole gabbronorite cumulates from Talkeetna (Greene et al., 2006)—are often the main host for sulfide mineralization in Alaskan-type orthomagmatic Ni-Cu-platinum group element (PGE) deposits found in arc-related settings (e.g., Thakurta et al., 2008; Piña et al., 2010). These deposits represent lower to midcrustal magmatic bodies that underwent extensive sulfide saturation and consequent segregation of magmatic sulfides that efficiently collect strongly chalcophile elements (Ripley and Li, 2013). As such, Cu-rich subarc cumulates that are proposed to account for the missing Cu in arc magmas, and arc-related orthomagmatic Ni-Cu-(PGE) deposits, could be viewed as part of a continuum of igneous processes. An increasingly recognized view for the genesis of arc-related Ni-Cu-(PGE) orthomagmatic deposits is that sulfide saturation is produced by the assimilation of reducing metasedimentary rocks, which in turn also contribute S to the system (Thakurta et al., 2008; Piña et al., 2010; Tomkins et al., 2012; Ripley and Li, 2013; Wei et al., 2019; Cao et al., 2020). Thus, the formation of Ni-Cu-(PGE) deposits provides an extreme example of the potential effects that crustal assimilation can have on the behavior of S and chalcophile elements during the evolution of arc magmas.

Here we show that the most primitive and Cu-rich Acadian cumulates assimilated metasedimentary rocks containing abundant graphite and sulfides (Figs. 5, 6). Because of its multivalent and redox-sensitive behavior, carbon (C) in assimilated graphite is a powerful agent to reduce the f_{O_2} of magmas. The oxidation of 1 mol of C to CO_2 can lead to the reduction of 4 mol of Fe^{3+} to Fe^{2+}, thus substantially decreasing the Fe^{3+}/Fe_{tot} ratio of the melt, which in turn leads to lower S solubility (Kress and Carmichael, 1991; Jugo, 2009). For instance, Tomkins et al. (2012) demonstrated that the assimilation of graphitic metasedimentary rocks by oxidized island-arc magmas can lead to a significant f_{O_2} drop, ultimately triggering sulfide precipitation and leading to the formation of orthomagmatic Ni-Cu-(PGE) deposits. We can place constraints on the f_{O_2} of the most primitive and Cu-rich Acadian cumulates to test the effects of crustal assimilation on the redox state of the magmatic system based on the olivine-orthopyroxene-spinel equilibrium assemblage. To do this, we used the experimentally calibrated parametrization of Mattioli and Wood (1988) and Wood and Virgo (1989), as recommended by Davis et al. (2017). Mineral compositions are given in Table 3. The activity of magnetite in spinel was calculated following Wood (1990). Pressure and temperature conditions are 1,000°C and 1 GPa (Tassara et al., 2021). Results indicate f_{O_2} values ranging from –2.5 to –1.9 (±0.3, from EPMA data) $\log_{10}$ units below the fayalite-magnetite-quartz buffer (ΔFMQ; Table 3). It is possible that the calculated f_{O_2} conditions represent minima due to subsolidus reequilibration during slow cooling and exhumation. However, such subsolidus f_{O_2} changes typically don't exceed more than an order of magnitude (Bucholz and Kelemen, 2019, and references therein). Therefore, even if subsolidus modifications altered the primary f_{O_2} of the rock, the obtained values are still indicative of reducing conditions. In addition, the calculated f_{O_2} conditions indicate that the rocks are significantly reduced compared to typical arc magmas (~ΔFMQ +1.3; Cottrell et al., 2021). This discrepancy is difficult to resolve without the involvement of reducing processes during the evolution of the parental magmas to the Acadian cumulates. Importantly, the calculated f_{O_2} conditions are comparable to those attained by calc-alkaline magmas of the Sierra Nevada batholith that assimilated graphite-bearing metasedimentary material (f_{O_2} at or below graphite saturation; Ague and Brimhall, 1987, 1988). These results show that the f_{O_2} of the Acadian cumulates is consistent with the assimilation of reducing metasedimentary rocks.

In summary, on the basis of field observations and S isotope systematics, we suggest that the Cu enrichment in the Acadian subarc cumulates was produced by extensive sulfide saturation triggered by the assimilation of reducing metasedimentary crust (Fig. 7). Assimilation-driven sulfide saturation after deep melt-crust interaction may be a widespread process in thickened continental arc crusts above subduction zones where orogenic growth extends the degree to which magmas interact with underthrusted and older crustal materials during ascent and differentiation. This mechanism has been

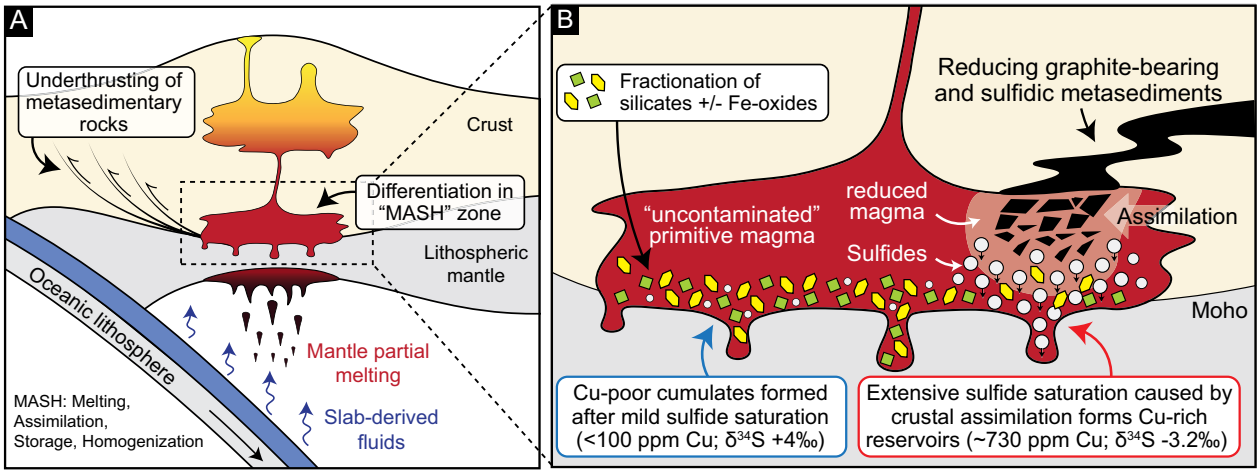

Fig. 7. Simplified geologic model of the tectonic (A) and petrogenetic (B) processes involved in the formation of the Cu-rich Acadian cumulates. (A) Ascent of primary magmas to the base of the lithosphere where they pond and begin to fractionate in a MASH zone. Deep-reaching thrust faults put metasedimentary rocks at deep crustal levels. (B) Assimilation of graphite-bearing sulfidic metasedimentary rocks with light S isotope compositions ($\delta^{34}S$ –19.5 to –12‰) causes a drop in oxygen fugacity, extensive sulfide saturation, and the formation of Cu-rich subarc hydrous cumulates with light S isotope signatures (~$\delta^{34}S$ –3‰); batches of similar magmas differentiate with less to no crustal assimilation and experiencing mild sulfide saturation leading to the formation of mafic cumulates with isotopically heavy S isotope compositions, disseminated sulfides, and low Cu contents.

previously suggested to produce the formation of orthomagmatic Ni-Cu-(PGE) deposits in island-arc settings (Tomkins et al., 2012). We emphasize that assimilation-driven sulfide saturation may also occur in thick continental arcs and need not operate alone but can work in combination with other processes such as the evolving nature of calc-alkaline magmas (i.e., Fe depletion) and decreasing temperature during ascent to promote and increase sulfide saturation.

Implications for the Genesis of Porphyry Copper Deposits

The nature of the deep crustal processes driving the evolution of magmas in subduction zones and how they impact the genesis and distribution of porphyry Cu deposits continues to be a matter of vigorous debate. In particular, the triggers and timing of sulfide saturation relative to fluid exsolution during magmatic evolution have long been recognized as a linchpin for many emerging hypotheses. The traditional view is that early sulfide saturation is detrimental to the development of porphyry Cu systems because it limits the amounts of ore-forming elements that can be delivered to shallow crustal levels and be transferred to mineralizing hydrothermal fluids (Jenner et al., 2010; Park et al., 2015, 2019; Richards, 2015; Hao et al., 2017). However, recent studies have shown that porphyry Cu deposits can form even if the parental magmas undergo some degree of sulfide saturation during ascent and evolution throughout the crust (Cocker et al., 2015; Hao et al., 2019; Du and Audétat, 2020; Park et al., 2021). In the latter case, it has been argued that small amounts of sulfide precipitation may considerably reduce the budget of strongly chalcophile and siderophile elements (e.g., Au and PGEs) but may not significantly affect other less chalcophile elements such as Cu, leading to evolved magmas with the potential to form Au-poor porphyry Cu deposits (e.g., Park et al., 2021). As such, what seems to be critical for the ore-forming potential of arc magmas is the amount of sulfide saturation they experienced and the extent to which sulfides were fractionated from the evolving magma. Therefore, if there is a particular process that can potentially produce anomalous degrees of sulfide precipitation, then this process will play a pivotal role in the fate of ore metals during magmatism and, therefore, in the ore fertility of magmas.

Our study provides direct evidence in support of the hypothesis that particularly large amounts of sulfide may precipitate when magmas interact with deeply buried reducing, graphite-bearing, metasedimentary crustal rocks (Fig. 7). In this scenario, the amount of precipitated sulfide is such that evolving magmas would lose their porphyry-forming potential at deep crustal levels. Thus, widespread graphite-bearing metasedimentary rocks—which can be identified by geoelectrical surveys because of their low resistivity—represent a crustal barrier to the flux of Cu and other chalcophile elements during arc magmatism, decreasing the ore-forming potential of magmas. We note that although the depth of erosion is also a factor to consider, this hypothesis may help explain the paucity of porphyry Cu deposits in the northern Appalachians. Paradoxically, it should also be noted that while extensive sulfide saturation driven by crustal assimilation limits the flux of ore-forming elements delivered to the shallow crust, it results in the formation of a deep Cu-rich reservoir. Although the Cu content of magmas may not need to be particularly high to form typical porphyry Cu deposits (Richards, 2015), it is clear that the more Cu that magmas have to transfer to the exsolved fluids, the greater the amount of Cu that can be concentrated during hydrothermal activity. As such, magmas parental to some giant porphyry Cu deposits (>2 millon tonnes of Cu) have been proposed to originate from anomalously Cu rich sources (e.g., Core et al., 2006; Richards, 2009; Wilkinson, 2013; Holwell et al., 2022). In this work, we show that extensive sulfide saturation following crustal assimilation is a viable mechanism to produce such Cu-rich sources in the lower crust. Subsequent remelting of these reservoirs or interaction

with ascending magmas in long-lived arcs or postsubduction settings could potentially trigger the formation of unusually Cu rich magmas.

Concluding Remarks

The studied hydrous ultramafic cumulates from the Acadian orogen in southern Central Maine terrane in New England (USA) provide a unique window into the early magmatic processes operating at the roots of continental arcs. They record major and trace element signatures of subduction zone magmatism and are complementary fractionated cumulates to the coeval calc-alkaline magmatism exposed elsewhere in the region. The Acadian cumulates are rich in Cu (up to ~730 μg g^{-1}) hosted by sulfide phases, indicating that the calc-alkaline parental magmas underwent sulfide saturation early during their petrogenetic evolution. Our data provide direct evidence for the formation of deep-seated Cu-rich reservoirs, showing that amphibole-dominated cumulates can be important sinks for Cu during the geochemical differentiation of calc-alkaline arc magmas and thus exert an important control on the flux of Cu and other chalcophile elements throughout continental-arc crusts. The initial S isotope composition of the parental magmas to the most primitive Acadian cumulates ($\delta^{34}S \approx -3‰$) deviates from mantle-like values and instead reflects assimilation of isotopically light S. Field relationships, S isotope systematics, and f_{O_2} estimates indicate that the most primitive and Cu-rich cumulates assimilated preexisting graphite-bearing reducing metasedimentary rocks (Fig. 7). We show that crustal assimilation was a key mechanism causing a significant drop in magmatic f_{O_2}, thus driving significant sulfide saturation and the consequent formation of subarc cumulates that are particularly enriched in Cu. Assimilation-driven sulfide saturation at the root of thickened arc crusts may be a common process controlling the formation and distribution of lower crust Cu-rich reservoirs. Consequently, the nature and distribution of reducing metasedimentary material in the deep crust of continental arcs may play a key role in the magmatic flux of S and chalcophile elements and, ultimately, on the formation and distribution of porphyry Cu deposits.

Acknowledgments

We thank D.S. Keller for insightful discussions and J.O. Eckert, Jr. for electron probe microanalysis assistance. We are grateful for financial support from Yale University through a Bateman Postdoctoral Fellowship to ST and from National Science Foundation awards EAR-0744154, EAR-1250269, and EAR-1753553 to JJA. Becker Construction Company kindly granted access to key exposures. We are thankful to Hongda Hao, Jia Chang, and an anonymous reviewer for their thoughtful evaluation of our study and to Veronique Le Roux for her comments on an earlier version of this paper. We also thank Associate Editor Andreas Audétat for excellent editorial handling and insightful comments on our work.

REFERENCES

Ague, J.J., and Brimhall, G.H., 1987, Granites of the batholiths of California: Products of local assimilation and regional-scale crustal contamination: Geology, v. 15, p. 63–66.

——1988, Magmatic arc asymmetry and distribution of anomalous plutonic belts in the batholiths of California: Effects of assimilation, crustal thickness, and depth of crystallization: Geological Society of America Bulletin, v. 100, p. 912–927.

Ague, J.J., Eckert, J.O., Jr., Chu, X., Baxter, E.F., and Chamberlain, C.P., 2013, Discovery of ultrahigh-temperature metamorphism in the Acadian orogen, Connecticut, US: Geology, v. 41, p. 271–274.

Alonso-Perez, R., Müntener, O., and Ulmer, P., 2009, Igneous garnet and amphibole fractionation in the roots of island arcs: Experimental constraints on andesitic liquids: Contributions to Mineralogy and Petrology, v. 157, p. 541–558.

Alt, J.C., Shanks, W.C., and Jackson, M.C., 1993, Cycling of sulfur in subduction zones: The geochemistry of sulfur in Mariana-island arc and back-arc trough: Earth and Planetary Science Letters, v. 119, p. 477–494.

Annen, C., Blundy, J.D., and Sparks, S.J., 2006, The genesis of intermediate and silicic magmas in deep crustal hot zones: Journal of Petrology, v. 47, p. 505–539.

Baker, D.R., and Moretti, R., 2011, Modeling the solubility of sulfur in magmas: A 50-year old geochemical challenge: Reviews in Mineralogy and Geochemistry, v. 73, p. 167–213.

Ballhaus, C., Tredoux, M., and Späth, A., 2001, Phase relations in the Fe-Ni-Cu-PGE-S system at magmatic temperature and application to massive sulfide ores of the Sudbury Igneous Complex: Journal of Petrology, v. 42, p. 1991–1926.

Barber, N.D., Edmonds, M., Jenner, F., Audétat, A., and Williams, H., 2021, Amphibole control on copper systematics in arcs: Insights from the analysis of global datasets: Geochimica et Cosmochimica Acta, v. 307, p. 192–211.

Barnes, S.J., 1986, The effect of trapped liquid crystallization on cumulus mineral compositions in layered intrusions: Contributions to Mineralogy and Petrology, v. 93, p. 524–531.

Behn, M.D., and Kelemen, P.B., 2006, Stability of arc lower crust: Insights from the Talkeetna arc section, south central Alaska, and the seismic structure of modern arcs: Journal of Geophysical Research: Solid Earth, v. 111, B11.

Bénard, A., Klimm, K., Woodland, A.B., Arculus, R.J., Wilke, M., Botcharnikov, R.E., Shimizu, N., Nebel, O., Rivard, C., and Ionov, D.A., 2018, Oxidising agents in sub-arc mantle melts link slab devolatilisation and arc magmas: Nature Communications, v. 9, p. 1–10.

Bucholz, C.E., and Kelemen, P.B., 2019, Oxygen fugacity at the base of the Talkeetna arc, Alaska: Contributions to Mineralogy and Petrology, v. 174, article 79.

Bucholz, C.E., Jagoutz, O., Schmidt, M.W., and Sambuu, O., 2014, Fractional crystallization of high-K arc magmas: Biotite- versus amphibole-dominated fractionation series in the Dariv Igneous Complex, Western Mongolia: Contributions to Mineralogy and Petrology, v. 168, article 1072.

Cao, Y., Wang, C.Y., and Wei, B., 2020, Magma oxygen fugacity of mafic-ultramafic intrusions in convergent margin settings: Insights for the role of magma oxidation states on magmatic Ni-Cu sulfide mineralization: American Mineralogist, v. 105, p. 1841–1856.

Cawthorn, R.G., 1996, Models for incompatible trace-element abundances in cumulus minerals and their application to plagioclase and pyroxenes in the Bushveld Complex: Contributions to Mineralogy and Petrology, v. 123, p. 109–115.

Chang, J., and Audétat, A., 2018, Petrogenesis and metal content of hornblende-rich xenoliths from two Laramide-age magma systems in southwestern USA: Insights into the metal budget of arc magmas: Journal of Petrology, v. 59, p. 1869–1898.

Chen, K., Tang, M., Lee, C-T.A., Wang, Z., Zou, Z., Hu, Z., and Liu, Y., 2020, Sulfide-bearing cumulates in deep continental arcs: The missing copper reservoir: Earth and Planetary Science Letters, v. 531, article 115971.

Chiaradia, M., 2014, Copper enrichment in arc magmas controlled by overriding plate: Nature Geoscience, v. 7, p. 43–46.

Chiaradia, M., Merino, D., and Spikings, R., 2009, Rapid transition to long-lived deep crustal magmatic maturation and the formation of giant porphyry-related mineralization (Yanacocha, Peru): Earth and Planetary Science Letters, v. 288, p. 505–515.

Chin, E.J., Shimizu, K., Bybee, G.M., and Erdman, M.E., 2018, On the development of the calc- alkaline and tholeiitic magma series: A deep crustal cumulate perspective: Earth and Planetary Science Letters, v. 482, p. 277–287.

Cocker, H.A., Valente, D.L., Park, J.W., and Campbell, I.H, 2015, Using platinum group elements to identify sulfide saturation in a porphyry Cu system: The El Abra porphyry Cu deposit, northern Chile: Journal of Petrology, v. 56, p. 2491–2514.

Core, D.P., Kesler, S.E., and Essene, E.J., 2006, Unusually Cu-rich magmas associated with giant porphyry copper deposits: Evidence from Bingham, Utah: Geology, v. 34, p. 41–44.

Cottrell, E., Birner, S.K., Brounce, M., Davis, F.A., Waters, L.E., and Kelley, K., 2021, Oxygen fugacity across tectonic settings: American Geophysical Union (AGU), Geophysical Monograph Series, v. 266, p. 33–61.

Cox, D., Watt, S.F.L., Jenner, F.E., Hastie, A.R., and Hammond, S.J., 2019, Chalcophile element processing beneath a continental arc stratovolcano: Earth and Planetary Science Letters, v. 522, p. 1–11.

Cox, D., Watt, S.F.L., Jenner, F.E., Hastie, A.R., Samantha, J.H., and Kunz, B., 2020, Elevated magma fluxes deliver high-Cu magmas to the upper crust: Geology, v. 48, p. 957–960.

Criss, R.E., 1999, Principles of stable isotope distribution: New York, Oxford University Press, 264 p.

Davidson, J., Turner, S., Handley, H., Macpherson, C., and Dosseto, A., 2007, Amphibole "sponge" in arc crust?: Geology, v. 35, p. 787–790.

Davis, F.A., Cottrell, E., Birner, S.K., Warren, J.M., and Lopez, O.G., 2017, Revisiting the electron microprobe method of spinel-olivine-orthopyroxene oxybarometry applied to spinel peridotites: American Mineralogist, v. 102, p. 421–435.

DeCelles, P.G., Ducea, M.N., Kapp, P., and Zandt, G., 2009, Cyclicity in cordilleran orogenic systems: Nature Geoscience, v. 2, p. 251–257.

de Hoog, J.C.M., Mason, P.R.D., and van Bergen, M.J., 2001, Sulfur and chalcophile elements in subduction zones: Constraints from a laser ablation ICP-MS study of melt inclusions from Galunggung volcano, Indonesia: Geochimica et Cosmochimica Acta, v. 65, p. 3147–3164.

DePaolo, D.J., 1981, Trace element and isotopic effects of combined wallrock assimilation and fractional crystallization: Earth and Planetary Science Letters, v. 53, p. 189–202.

Dessimoz, M., Müntener, O., and Ulmer, P., 2012, A case for hornblende dominated fractionation of arc magmas: The Chelan Complex (Washington Cascades): Contributions to Mineralogy and Petrology, v. 163, p. 567–589.

Dorais, M.J., 2003, The petrogenesis and emplacement of the New Hampshire Plutonic Suite: American Journal of Science, v. 303, p. 447–487.

Du, J., and Audétat, A., 2020, Early sulfide saturation is not detrimental to porphyry Cu-Au formation: Geology, v. 48, p. 519–524.

Ferrero, S., Ague, J.J., O'Brien, P.J., Wunder, B., Remusat, L., Ziemann, M.A., and Axler, J., 2021, High pressure, halogen-bearing melt preserved in ultra-high temperature felsic granulites of the Central Maine terrane, Connecticut (U.S.A.): American Mineralogist, v. 106, p. 1225–1236.

Fiege, A., Holtz, F., Shimizu, N., Mandeville, C.W., Behrens, H., and Knipping, J.L., 2014, Sulfur isotope fractionation between fluid and andesitic melt: An experimental study: Geochimica et Cosmochimica Acta, v. 142, p. 501–521.

Greene, A.R., DeBari, S.M., Kelemen, P.B., Blusztajn, J., and Clift, P.D., 2006, a detailed geochemical study of island arc crust: The Talkeetna arc section, south-central Alaska: Journal of Petrology, v. 47, p. 1051–1093.

Grocke, S.B., Cottrell, E., de Silva, S., and Kelley, K., 2016, The role of crustal and eruptive processes versus source variations in controlling the oxidation state of iron in Central Andean magmas: Earth and Planetary Science Letters, v. 440, p. 92–104.

Hao, H., Campbell, I.H., Park, J.-W., and Cooke, D.R., 2017, Platinum-group element geochemistry used to determine Cu and Au fertility in the Northparkes igneous suites, New South Wales, Australia: Geochimica et Cosmochimica Acta, v. 216, p. 372–392.

Hao, H., Campbell, I.H., Richards, J.P., Nakamura, E., and Sakaguchi, C., 2019, Platinum-group element geochemistry of the Escondida igneous suites, northern Chile: Implications for ore formation: Journal of Petrology, v. 60, p. 487–514.

Hatcher, R.D., Jr., 2010, The Appalachian orogen: A brief summary: Geological Society of America Memoirs, v. 206, p. 1–19.

Hedenquist, J.W., and Lowenstern, J.B., 1994, The role of magmas in the formation of hydrothermal ore deposits: Nature, v. 370, p. 519–527.

Hildreth, W., and Moorbath, S., 1988, Crustal contributions to arc magmatism in the Andes of Central Chile: Contributions to Mineralogy and Petrology, v. 98, p. 455–489.

Holwell, D.A., Fiorentini, M.L., Knott, T.R., McDonald, I., Blanks, D.E., McCuaig, T.C., and Gorczyk., W., 2022, Mobilisation of deep crustal sulfide melts as a first order control on upper lithospheric metallogeny: Nature Communications, v. 13, article 573.

Jagoutz, O., and Behn, M.D., 2013, Foundering of lower island-arc crust as an explanation for the origin of the continental Moho: Nature, v. 504, p. 131–134.

Jagoutz, O., Müntener, O., Schmidt, M.W., and Burg, J.-P., 2011, The roles of flux and decompression melting and their respective fractionation lines for continental crust formation: Evidence from the Kohistan arc: Earth and Planetary Science Letters, v. 303, p. 25–36.

Jenner, F.E., 2017, Cumulate causes for the low contents of sulfide-loving elements in the continental crust: Nature Geoscience, v. 10, p. 524–529.

Jenner, F.E., O'Neill, H.S.C., Arculus, R.J., and Mavrogenes, J.A., 2010, The magnetite crisis in the evolution of arc-related magmas and the initial concentration of Au, Ag and Cu: Journal of Petrology, v. 51, p. 2445–2464.

Jugo, P.J., 2009, Sulphur content at sulphide saturation in oxidized magmas: Geology, v. 37, p. 415–418.

Kelemen, P.B., Hanghøj, K., and Greene, A.R., 2007, One view of the geochemistry of subduction-related magmatic arcs, with an emphasis on primitive andesite and lower crust, *in* Rudnick, R.L., ed., Treatise on geochemistry, v. 3: Elsevier, p. 593–659.

Keller, D.S., and Ague, J.J., 2018, High-pressure granulite facies metamorphism (~1.8 GPa) revealed in silica-undersaturated garnet-spinel-corundum gneiss, Central Maine terrane, Connecticut, USA: American Mineralogist, v. 103, p. 1851–1868.

——2020, Quartz, mica, and amphibole exsolution from majoritic garnet reveals ultra-deep sediment subduction, Appalachian orogen: Science Advances, v. 6, eaay5178.

Kress, V.C., and Carmichael, I.S.E., 1991, The compressibility of silicate liquids containing Fe_2O_3 and the effect of composition, temperature, oxygen fugacity and pressure on their redox states: Contributions to Mineralogy and Petrology, v. 108, p. 82–92.

Labidi, J., and Cartigny, P., 2016, Negligible sulfur isotope fractionation during partial melting: Evidence from Garrett transform fault basalts, implications for the late-veneer and the hadean matte: Earth and Planetary Science Letters, v. 451, p. 197–207.

Labidi, J., Cartigny, P., Birck, J.L., Assayag, N., and Bourrand, J.J., 2012, Determination of multiple sulfur isotopes in glasses: A reappraisal of the MORB $\delta^{34}S$: Chemical Geology, v. 334, p. 189–198.

Larocque, J., and Canil., D., 2010, The role of amphibole in the evolution of arc magmas and crust: The case from the Jurassic Bonanza arc section, Vancouver Island, Canada: Contributions to Mineralogy and Petrology, v. 159, p. 475–492.

Lee, C.-T.A., Luffi, P., Chin, E.J., Bouchet, R., Dasgupta, R., Morton, D.M., Le Roux, V., Yin, Q.-Z., and Jin, D., 2012, Copper systematics in arc magmas and implications for crust-mantle differentiation: Science, v. 336, p. 64–68.

Lee, C-T.A., Erdman, M., Yang, W., Ingram, L., Chin, E.J., and DePaolo, J.D., 2018, Sulfur isotopic compositions of deep arc cumulates: Earth and Planetary Science Letters, v. 500, p. 76–85.

Li, C., and Ripley, E.M., 2005, Empirical equations to predict the sulfur content of mafic magmas at sulfide saturation and applications to magmatic sulfide deposits: Mineralium Deposita, v. 40, p. 218–230.

Li, J-L., Schwarzenbach, E.M., John, T., Ague, J.J., Huang, F., Gao, J., Klemd, R., Whitehouse, M.J., and Wang, X-S., 2020, Uncovering and quantifying the subduction zone sulfur cycle from the slab perspective: Nature Communications, v. 11, article 514.

Li, J-L., Schwarzenbach, E.M., John, T., Ague, J.J., Tassara, S., Gao, J., and Konecke, B.A., 2021, Subduction zone sulfur mobilization and redistribution by intraslab fluid-rock interaction: Geochimica et Cosmochimica Acta, v. 297, p. 40–64.

Li, J-Y., Tang, M., Lee, C-T.A., Wang, X-L., Gu, Z-G., Xia, X-P., Wang, D., Du, D-H., and Li, L-S., 2021, Rapid endogenic rock recycling in magmatic arcs: Nature Communications, v. 12, article 3533.

Li, Y., Audétat, A., Liu, Z., and Wang, F., 2021, Chalcophile element partitioning between Cu-rich sulfide phases and silicate melt and implications for the formation of Earth's continental crust: Geochimica et Cosmochimica Acta, v. 302, p. 61–82.

Liu, Y., Samaha, N-T., and Baker, D.R., 2007, Sulfur concentration at sulfide saturation (SCSS) in magmatic silicate melts: Geochimica et Cosmochimica Acta, v. 71, p. 183–1799.

Mandeville, C.W., Webster, J.D., Tappen, C., Taylor, B.E., Timbal, A., Sasaki, A., Hauri, E., and Bacon, C.R., 2009, Stable isotope and petrologic evidence for open-system degassing during the climactic and pre-climactic eruptions of Mt. Mazama, Crater Lake, Oregon: Geochimica et Cosmochimica Acta, v. 73, p. 2978–3012.

Marini, L., Moretti, R., and Accornero, M., 2011, Sulfur isotopes in magmatic-hydrothermal systems, melts, and magmas: Reviews in Mineralogy and Geochemistry, v. 73, p. 423–492.

Matjuschkin, V., Blundy, J.D., and Brooker, R.A., 2016, The effect of pressure on sulphur speciation in mid- to deep-crustal arc magmas and implications for the formation of porphyry copper deposits: Contributions to Mineralogy and Petrology, v. 171, article 66.

Mattioli, G.S., and Wood, B.J., 1988, Magnetite activities across the $MgAl_2O_4$-Fe_3O_4 spinel join, with application to thermobarometric estimates of upper mantle oxygen fugacity: Contributions to Mineralogy and Petrology, v. 98, p. 148–162.

Mavrogenes, J.A., and O'Neill, H.S.C., 1999, The relative effects of pressure, temperature and oxygen fugacity on the solubility of sulfide in mafic magmas: Geochimica et Cosmochimica Acta, v. 63, p. 1173–1180.

McDonough, W.F., and Sun, S.-S., 1995, The composition of the Earth: Chemical Geology, v. 120, p. 223–253.

Métrich, N., Schiano, P., Clocchiatti, R., and Maury, R.C., 1999, Transfer of sulfur in subduction settings: An example from Batan Island (Luzon volcanic arc, Philippines): Earth and Planetary Science Letters, v. 167, p. 1–14.

Müntener, O., and Ulmer, P., 2018, Arc crust formation and differentiation constrained by experimental petrology: American Journal of Science, v. 318, p. 64–89.

Müntener, O., Kelemen, P.B., and Grove, T.L., 2001, The role of H_2O during crystallization of primitive arc magmas under uppermost mantle conditions and genesis of igneous pyroxenites: An experimental study: Contributions to Mineralogy and Petrology, v. 141, p. 643–658.

Muth, M.J., and Wallace, P.J., 2021, Slab-derived sulfate generates oxidized basaltic magmas in the southern Cascade arc (California, USA): Geology, v. 49, p. 1177–1181.

Ohmoto, H., and Rye, R.O., 1979, Isotopes of sulfur and carbon, *in* Barnes, H.L., ed., Geochemistry of hydrothermal ore deposits: Wiley, p. 509–567.

O'Neill, H.S.C., and Mavrogenes, J.A., 2002, The sulfide capacity and sulfur content at sulfide saturation of silicate melts at 1400°C and 1 bar: Journal of Petrology, v. 43, p. 1049–1087.

Park, J.-W., Campbell, I.H., Kim, J., and Moon, J.-W., 2015, The role of late sulfide saturation in the formation of a Cu- and Au-rich magma: Insights from the platinum-group geochemistry of Niuatahi-Motutahi lavas, Tonga rear arc: Journal of Petrology, v. 56, p. 59–81.

Park, J.-W., Campbell, I.H., Malaviarachchi, S.P.K., Cocker, H., Hao, H., and Kay, S.M., 2019, Chalcophile element fertility and the formation of porphyry Cu ± Au deposits: Mineralium Deposita, v. 54, p. 657–670.

Park, J.-W., Campbell, I.H., Chiaradia, M., Hao, H., and Lee, C-T., 2021, Crustal magmatic controls on the formation of porphyry copper deposits: Nature Reviews Earth and Environment, v. 2, p. 542–557.

Phillipots, A.R., and Ague, J.J., 2009, Principles of igneous and metamorphic petrology: New York, Cambridge University Press, 667 p.

Piña, R., Romeo, I., Ortega, L., Lunar, R., Capote, R., Gervilla, F., Tejero, R., and Quesada, C., 2010, Origin and emplacement of the Aguablanca magmatic Ni-Cu-(PGE) sulfide deposit, SW Iberia: A multidisciplinary approach: Geological Society of America Bulletin, v. 122, p. 915–925.

Putirka, K.D., 2008, Thermometers and barometers for volcanic systems: Reviews in Mineralogy and Geochemistry, v. 69, p. 61–120.

Rezeau, H., and Jagoutz, O., 2020, The importance of H_2O in arc magmas for the formation of porphyry Cu deposits: Ore Geology Reviews, v. 126, article 103744.

Richards, J.P., 2003, Tectono-magmatic precursors for porphyry Cu-(Mo-Au) deposit formation: Economic Geology, v. 98, p. 1515–1533.

——2009, Postsubduction porphyry Cu-Au and epithermal Au deposits: Products of remelting of subduction-modified lithosphere: Geology, v. 37, p. 247–250.

——2015, The oxidation state, and sulfur and Cu contents of arc magmas: Implications for metallogeny: Lithos, v. 233, p. 27–45.

Rickard, D., 2014, The sedimentary sulfur system: Biogeochemistry and evolution through geologic time, *in* Mackenzie, F.T., ed., Treatise on geochemistry, v. 9: Sediments, diagenesis and sedimentary rocks: Elsevier, p. 267–326.

Ripley, E.M., and Li, C., 2013, Sulfide saturation in mafic magmas: Is external sulfur required for magmatic Ni-Cu-(PGE) ore genesis?: Economic Geology, v. 108, p. 45–48.

Rodgers, J., 1985, Bedrock geological map of Connecticut: Connecticut Geological and Natural History Survey, Connecticut Natural Resources Atlas Series, scale 1:125,000.

Saal, A.E., Rudnick, R.L., Ravizza, G.E., and Hart, S.R., 1998, Re-Os isotope evidence for the composition, formation and age of the lower continental crust: Nature, v. 393, p. 58–61.

Schmidt, M.W., and Jagoutz, O., 2017, The global systematics of primitive arc melts: Geochemistry, Geophysics, Geosystems, v. 18, p. 2817–2854.

Sillitoe, R.H., 1972, A plate tectonic model for the origin of porphyry copper deposits: Economic Geology, v. 67, p. 184–197.

——2010, Porphyry copper systems: Economic Geology, v. 105, p. 3–41.

——2012, Copper provinces: Society of Economic Geologists, Special Publication 16, p. 1–18.

Smith, D.J., 2014, Clinopyroxene precursors to amphibole sponge in arc crust: Nature Communications, v. 5, article 4329.

Tassara, S., González-Jiménez, J.M., Reich, M., Saunders, E., Luguet, A., Morata, D., Grégoire, M., van Acken, D., Schilling, M.E., Barra, F., Nowell, G., and Corgne, A., 2018, Highly siderophile elements mobility in the subcontinental lithospheric mantle beneath southern Patagonia: Lithos, v. 314–315, p. 579–596.

Tassara, S., Ague, J.J., and Valencia, V., 2021, The deep magmatic cumulate roots of the Acadian orogen, eastern North America: Geology, v. 49, p. 168–173.

Taylor, H.P., Jr., 1980, The effects of assimilation of country rocks by magmas on $^{18}O/^{16}O$ and $^{87}Sr/^{86}Sr$ systematics in igneous rocks: Earth and Planetary Science Letters, v. 47, p. 243–254.

Taylor, H.P., Jr., and Sheppard, S.M.F., 1986, Igneous rocks: I: Processes of isotopic fractionation and isotope systematics: Reviews in Mineralogy, v. 16, p. 277–271.

Thakurta, J., Ripley, E.M., and Li, C., 2008, Geochemical constraints on the origin of sulfide mineralization in the Duke Island Complex, southeastern Alaska: Geochemistry, Geophysics, Geosystems, v. 9, Q07003.

Tomkins, A.G., Rebryna, K.C., Weinberg, R.F., and Schaefer, B.F., 2012, Magmatic sulfide formation by reduction of oxidized arc basalt: Journal of Petrology, v. 53, p. 1537–1567.

van Staal, C.R., Whalen, J.B., Valverde-Vaquero, P., Zagorevski, A., and Rogers, N., 2009, Pre-Carboniferous, episodic accretion-related, orogenesis along the Laurentian margin of the northern Appalachians: Geological Society, London, Special Publication 327, p. 271–316.

Velázquez Santana, L.C., McLeod, C.L., Blakemore, D., Shaulis, B., and Hill, T., 2020, Bolivian hornblendite cumulates: Insights into the depths of Central Andean arc magmatic systems: Lithos, v. 370–371, article 105618.

Walker, B.A., Jr., Bergantz, G.W., Otamendi, J.E., Ducea, M.N., and Cristofolini, E.A., 2015, A MASH zone revealed: The mafic complex of the Sierra Valle Fértil: Journal of Petrology, v. 56, 1863–1896.

Wallace, P.J., and Edmonds, M., 2011, The sulfur budget in magmas: Evidence from melt inclusions, submarine glasses, and volcanic gas emissions: Reviews in Mineralogy and Geochemistry, v. 73, p. 215–246.

Walters, J.B., Cruz-Uribe, A.M., and Marschall, H.R., 2019, Isotopic compositions of sulfides in exhumed high-pressure terranes: Implications for sulfur cycling in subduction zones: Geochemistry, Geophysics, Geosystems, v. 20, p. 3347–3374.

Wang, Z., Becker, H., Liu, Y., Hoffmann, E., Chen, C., Zou, Z., and Li, Y., 2018, Constant Cu/Ag in upper mantle and oceanic crust: Implications for the role of cumulates during the formation of continental crust: Earth and Planetary Science Letters, v. 493, p. 25–35.

Wei, B., Wang, C.Y., Lahaye, Y., Xie, L., and Cao, Y., 2019, S and C isotope constraints for mantle-derived sulfur source and organic carbon-induced sulfide saturation of magmatic Ni-Cu sulfide deposits in the Central Asian orogenic belt, North China: Economic Geology, v. 114, p. 787–806.

Wilkinson, J.J., 2013, Triggers for the formation of porphyry ore deposits in magmatic arcs: Nature Geoscience, v. 6, p. 917–925.

Wood, B.J., 1990, An experimental test of the spinel peridotite oxygen barometer: Journal of Geophysical Research, v. 95, p. 845–851.

Wood, B.J., and Virgo, D., 1989, Upper mantle oxidation state: Ferric iron contents of lherzolite spinels by ^{57}Fe Mössbauer spectroscopy and resultant oxygen fugacities: Geochimica et Cosmochimica Acta, v. 53, p. 1277–1291.

Zhou, J-S., Yang, Z-S., Hou, Z-Q., and Wang, Q., 2020, Amphibole-rich cumulate xenoliths in the Zhazhalong intrusive suite, Gangdese arc: Implications for the role of amphibole fractionation during magma evolution: American Mineralogist, v. 105, p. 262–275.

Santiago Tassara focuses on the magmatic and tectonic processes that control the formation and regional-scale distribution of large base and precious metal deposits and metallogenic provinces. In particular, his work aims at providing a comprehensive understanding of the behavior and flux of ore-forming elements during magmatism as a solid basis that serves to improve and develop cutting-edge exploration strategies. He has shaped his academic training at the National University of La Plata, Argentina (B.Sc.), the University of Barcelona (M.Sc.), the University of Chile (Ph.D.), and more recently at Yale University, where he held a Bateman Postdoctoral Fellowship.

Jay Ague studies the metamorphic and igneous rocks constituting the deep roots of mountain belts, focusing on heat and fluid transport through rocks and implications for earthquake hazards, volcanism, economic mineral deposits, and the roles of mountain building and subduction in global carbon and climate cycles. He earned his B.S. and M.S. degrees from Wayne State University and his Ph.D. from UC Berkeley. He joined Yale University as an assistant professor and is now the Henry Barnard Davis Memorial Professor of Earth and Planetary Sciences and the curator in charge of mineralogy and meteoritics at the Yale Peabody Museum of Natural History.